Supporting Information for

Structural setting of the Sixtymile gold prospect, Yukon, Canada: Insights from field-mapping and 3D magnetic inversion

Jeremy Rimando[1], Alexander Peace[1], Meixia Geng[2], Jaap Verbaas[3] and Harley Slade[3]

[1] School of Earth, Environment and Society, McMaster University, Hamilton, Ontario, Canada
[2] Department of Earth Sciences, Khalifa University of Science and Technology, Abu Dhabi, United Arab Emirates
[3] Flow Metals Corporation, Vancouver, British Columbia, Canada
* Correspondence: rimandoj@mcmaster.ca

Contents of this file

Text S1-S4

Figures S1-S36

Tables S1 & S2

Introduction

This supporting information provides location maps for drillholes and figures showing key hand specimen and thin sections. Data from both diamond and rotary airblast (RAB) drilling (**Figure S1-S9**) were used to augment surface mapping of the geology (**Figure S10-S36**). Along with logs from diamond drilling and rotary airblast (RAB) drilling, hand specimen and thin sections were used to characterize the formations, and corresponding lithologies, in this study.

Text S1. Upper Devonian to Mississippian Finlayson Group carbonaceous metasedimentary rocks (DMF3)

DDH-11-18 (103.82 m - 106.97 m; **Figs. S1, S3 & S10**), is a medium-grained, quartz-rich quartz muscovite schist. It is worth noting that despite being geographically contained within the DMF3, which includes the Nasina Schist (Yukon Geological Survey (2020), this lithologic description is typically classified by Slade (2020) as Klondike Schist. Logs of the entire interval of core ranging from 103.82 m - 106.97 m describe DDH-11-18 (**Figure S10**) as exhibiting discontinuous stringers of pyrite, quartz veining with blebby arsenopyrite and pyrite, minor sphalerite. Alteration includes siliceous zones

and sericitization along with local/minor kaolinite and limonite on fracture surfaces. Structures observed include undulating foliation and foliation-parallel quartz veins.

Text S2. Middle to Late Permian Klondike Schist (PK2)

DDH-11-15 (**Figs. S1, S3 & S11-S15**), and DDH-11-20 (**Figs. S1, S5, 16 & 17**), are generally strongly foliated, fine- to coarse-grained muscovite quartz schists, including varying amounts of chlorite and biotite. Logs of the entire interval of core of DDH-11-15 ranging from 194.97 m to 199.30 m (**Figure S1, S3 & S11**) and 224.9 m to 233.33 m (**Figs. S1, S3 & S11-S15**) are described in drill reports as exhibiting visible gold (2-3mm sized gold specs within a quartz vein between 229.38m - 229.4 m), blebby arsenopyrite, and stringers/veins of pyrite and hematite. Alteration includes pervasive silicification, sericitization and chloritization. Core logs describe DDH-11-20 (166.10 m - 170.14 m; **Figs. S1, S5, 16 & 17**) as having quartz- and quartz-carbonate veins with pyrite ± hematite.

Text S3. Upper Devonian to Mississippian Finlayson Group intermediate to mafic volcanic and volcaniclastic rocks, and fine-grained amphibolite and greenstone (DMF1)

DDH-11-01 (**Figs. S1, S2 & S18**), DDH-11-02 (**Figs. S1, S2, S19 & S20**), and DDH-11-10 (**Figs. S1, S2, S21 & S22**) are generally medium-grained schists, with variety of compositions. DDH-11-01 (165.51 m - 169.65 m; **Figs. S1, S2 & S18**) is a feldspar-biotite-amphibole-quartz schist with blebby and fracture-fill pyrite, which exhibits pervasive sericitization. DDH-11-02 (130.67 m - 135.05 m; **Figs. S1, S2, S19 & S20**), and DDH-11-02 (135.05 m - 139.34 m; **Figs. S1, S2, S19 & S20**) are chlorite-mica schists with blebby, disseminated, stringer/vein-related, and fracture-fill pyrite, which exhibit pervasive propylitic alteration and fracture related oxidation. DDH-11-02 exhibits strong foliation with minor quartz augens and localized crenulation cleavage. DDH-11-10 (247.69 m - 251.34 m; **Figs. S1, S2, S21 & S22**) is a quartz-biotite schist with disseminated hematite, and both stringer/vein-related

and disseminated pyrite, which exhibits pervasive silicification, fracture-related argillization, and overprints of chloritization and oxide alteration.

Text S4. Upper Cretaceous Carmacks Group

DDH-11-03 (**Figs. S1, S2 & S23-S25**), DDH-11-05 (**Figs. S1, S2, S26 &S27**), DDH-11-07 (**Figs. S1, S2 & S28-S30**), DDH-11-08 (**Figs. S1, S2, S31 & S32**), DDH-11-16 (**Figs. S1, S2, S33 & S34**), and DDH-11-17 (**Figs. S1, S2, S35 & S36**) are generally fine- to coarse-grained porphyritic andesites which are mostly highly fractured, and locally brecciated. Fault and flow breccia was observed in DDH-11-16 (**Figs. S1, S2, S33 & S34**), while hydrothermal breccia was observed in DDH-11-07 (**Figs. S1, S2 & S28-S30**) and DDH-11-08 (**Figs. S1, S2, S31 & S32**). Core logs generally describe these samples as exhibiting mostly fracture-fill, disseminated, and stringer/vein-related pyrite; rarely containing hematite and galena. A wide variety of alteration can be observed in the porphyritic andesites of the Upper Cretaceous Carmacks Group, including localized-to-pervasive sericitization (DDH-11-03: **Figs. S1, S2 & S23-S25**; DDH-11-17; **Figs. S1, S2, S35 & S36**), pervasive silicification (DDH-11-05; **Figs. S1, S2 & S26-S27**), fracture-related silicification (DDH-11-07; **Figs. S1, S2 & S28-S30**), over-printed silicification (DDH-11-07: **Figs. S1, S2 & S28-S30**; DDH-11-08: **Figs. S1, S2, S31 & S32**; and DDH-11-17: **Figs. S1, S2, S35 & S36**) potassic alteration DDH-11-03 (**Figs. S1, S2 & S23-S25**), argillization (DDH-11-16: **Figs. S1, S2, S33 & S34**; and DDH-11-17: **Figs. S1, S2, S35 & S36**), oxidation (DDH-11-16; **Figs. S1, S2, S33 & S34**). Quartz and dolomite veins were documented in DDH-11-08 (**Figs. S1, S2, S31 & S32**), while calcite veins were observed in DDH-11-16 (**Figs. S1, S2, S33 & S34**). Remarkably, DDH-11-17 (**Figs. S1, S2, S35 & S36**) exhibits a slightly schistose texture.

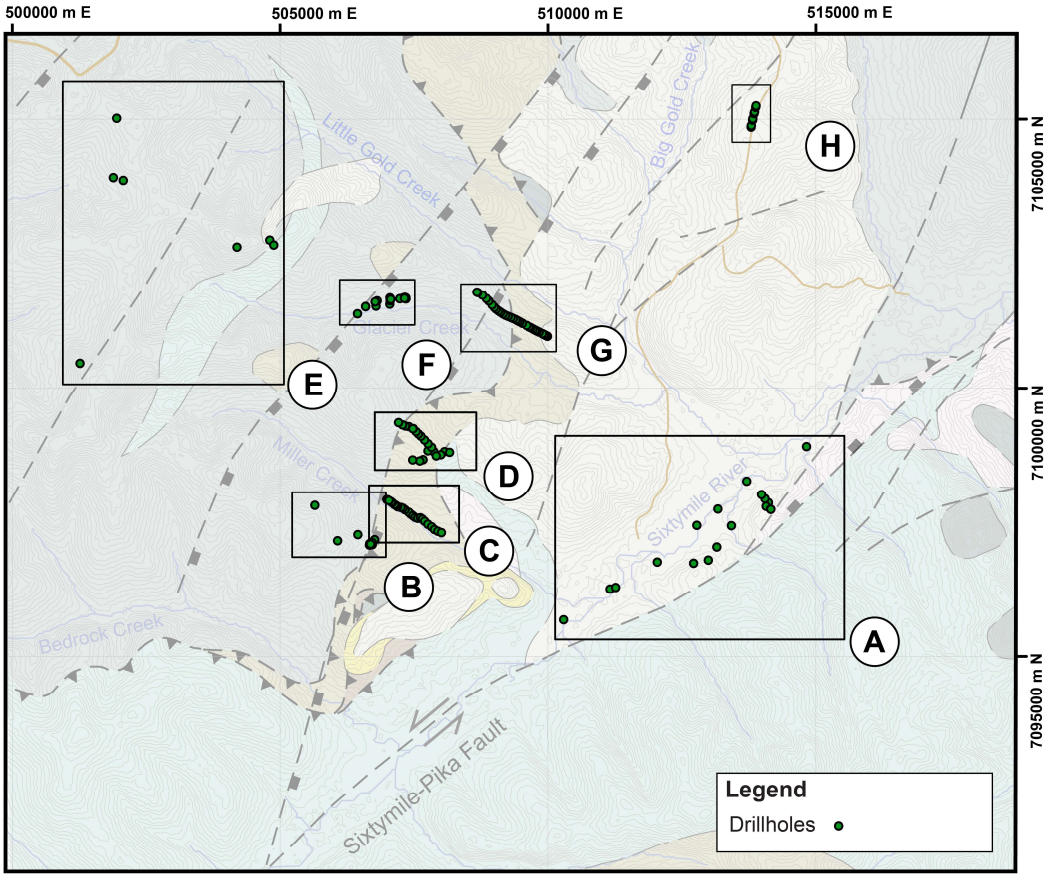

Figure S1. Drillhole location map. Boxes A-H correspond to larger scale drillhole location maps (**Appendix Figs. S2-S9**).

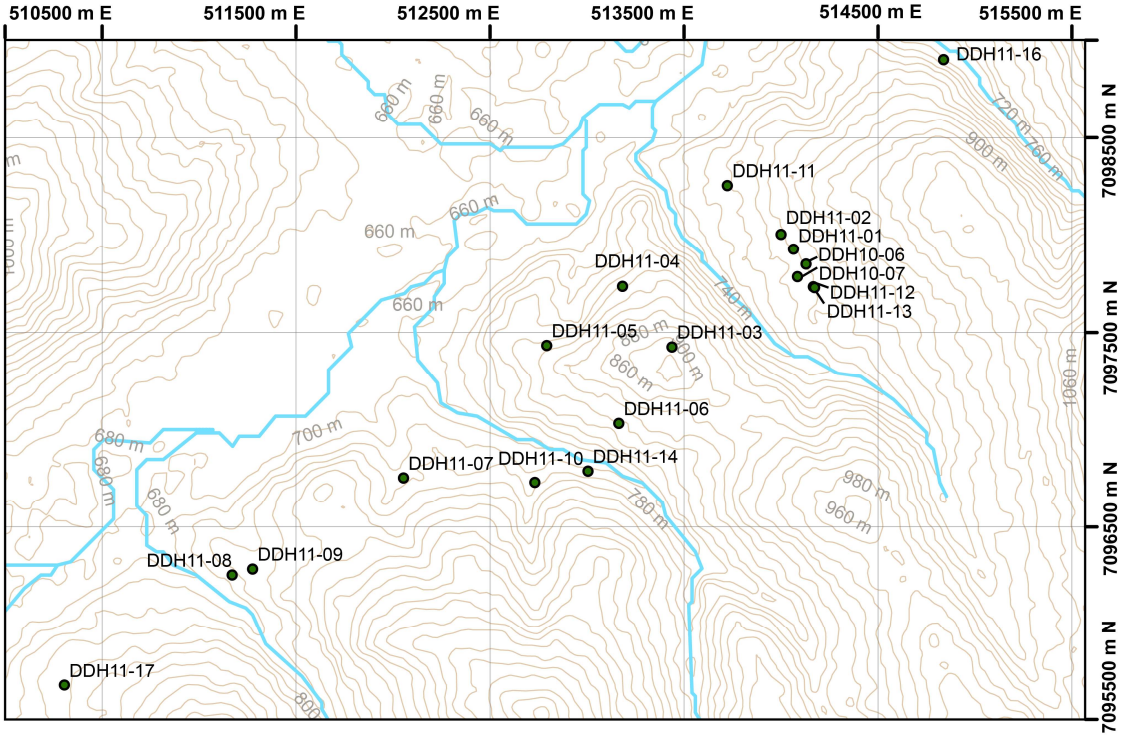

Figure S2. Drillhole location map A. Refer to Supplementary Figure S1. for this map's location within the Sixtymile District.

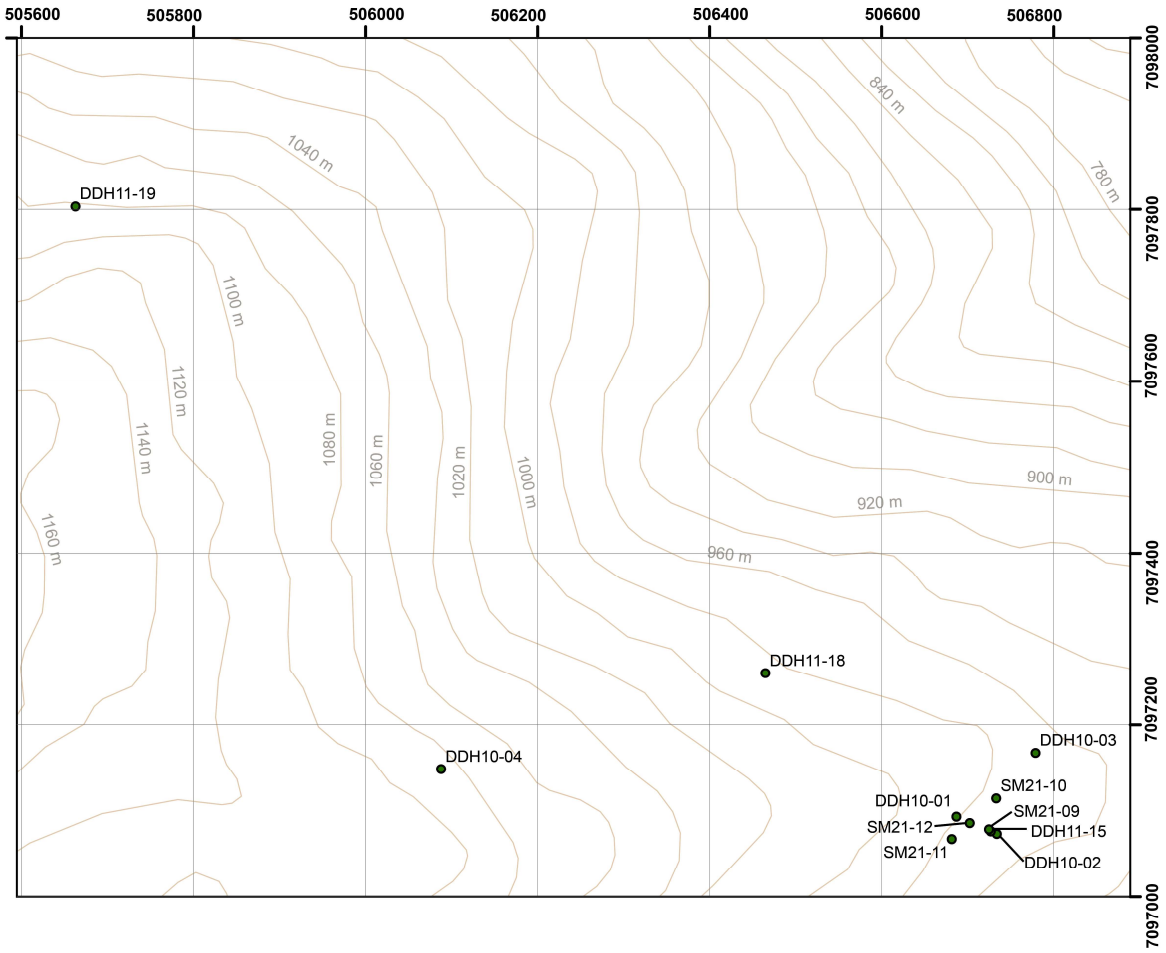

Figure S3. Drillhole location map B. Refer to Supplementary Figure S1. for this map's location within the Sixtymile District.

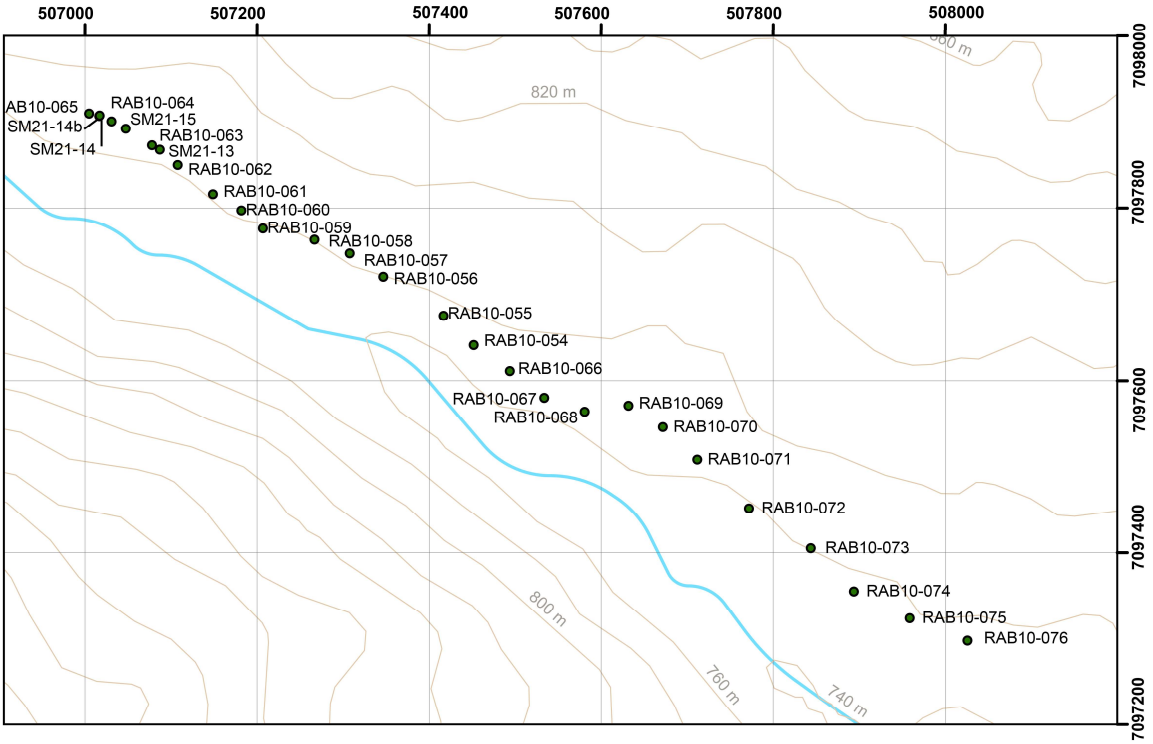

Figure S4. Drillhole location map C. Refer to Supplementary Figure S1. for this map's location within the Sixtymile District.

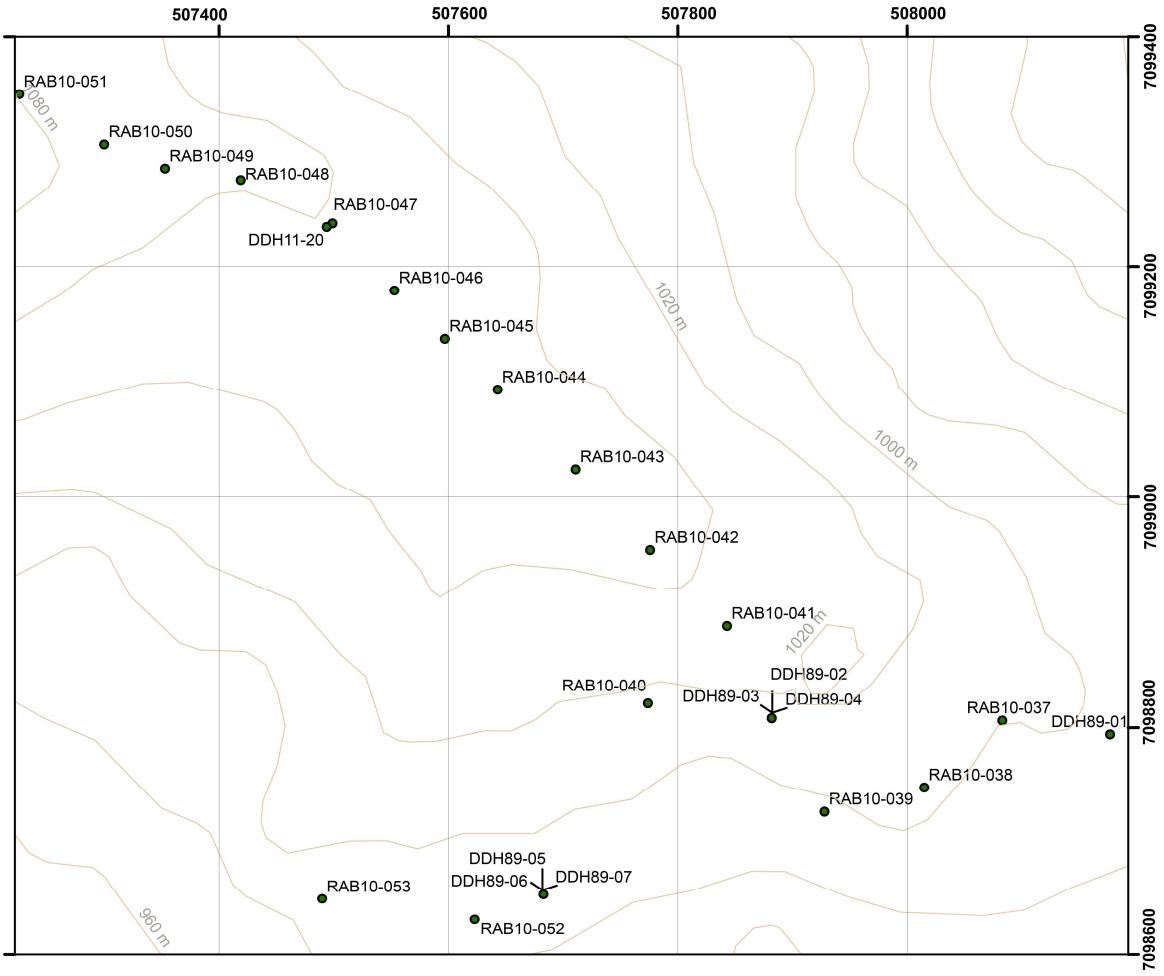

Figure S5. Drillhole location map D. Refer to Supplementary Figure S1. for this map's location within the Sixtymile District.

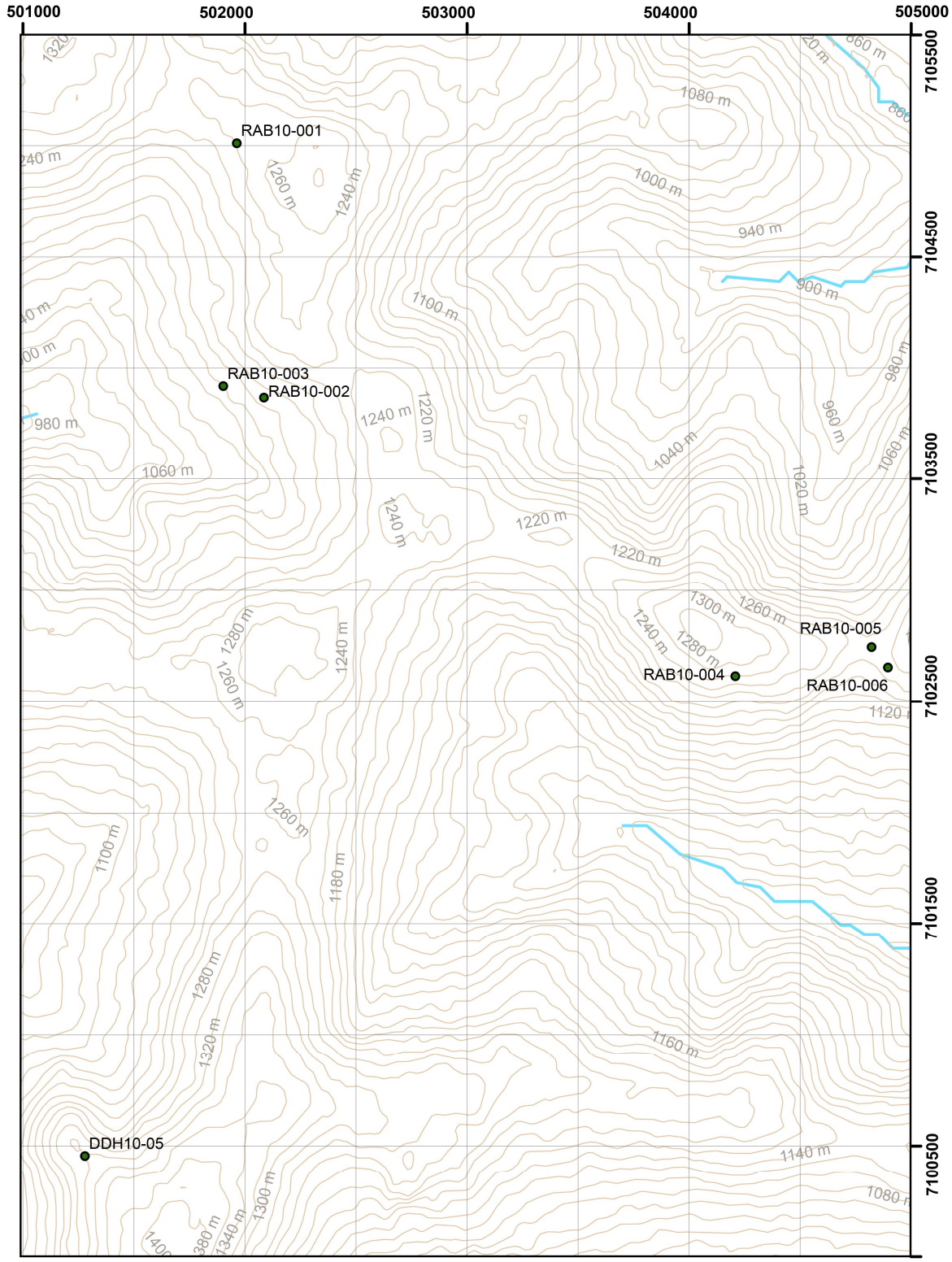

Figure S6. Drillhole location map E. Refer to Supplementary Figure S1. for this map's location within the Sixtymile District.

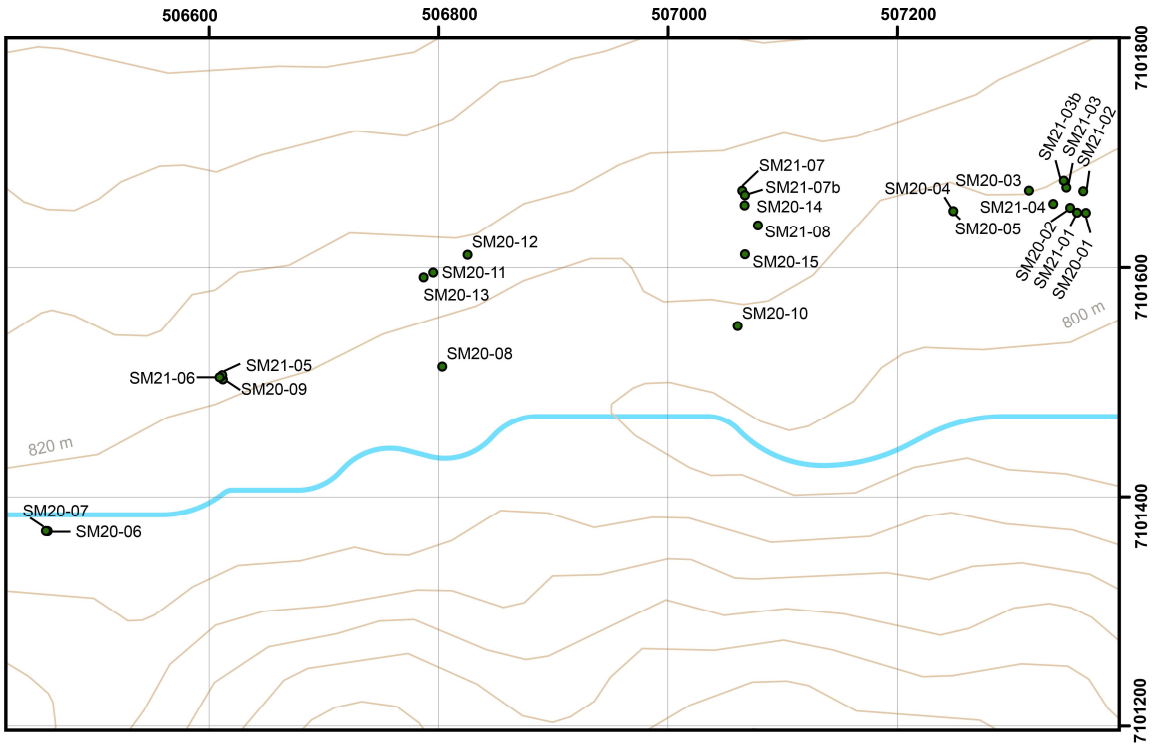

Figure S7. Drillhole location map F. Refer to Supplementary Figure S1. for this map's location within the Sixtymile District.

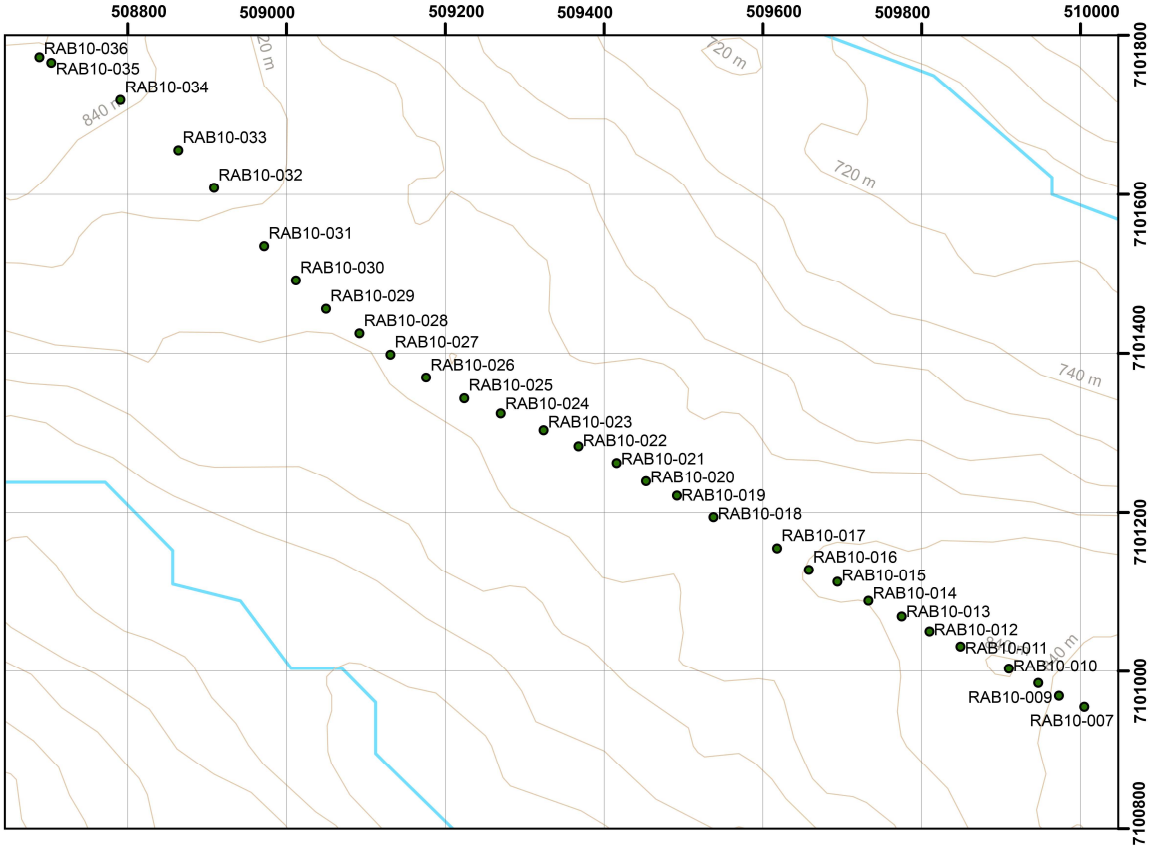

Figure S8. Drillhole location map G. Refer to Supplementary Figure S1. for this map's location within the Sixtymile District.

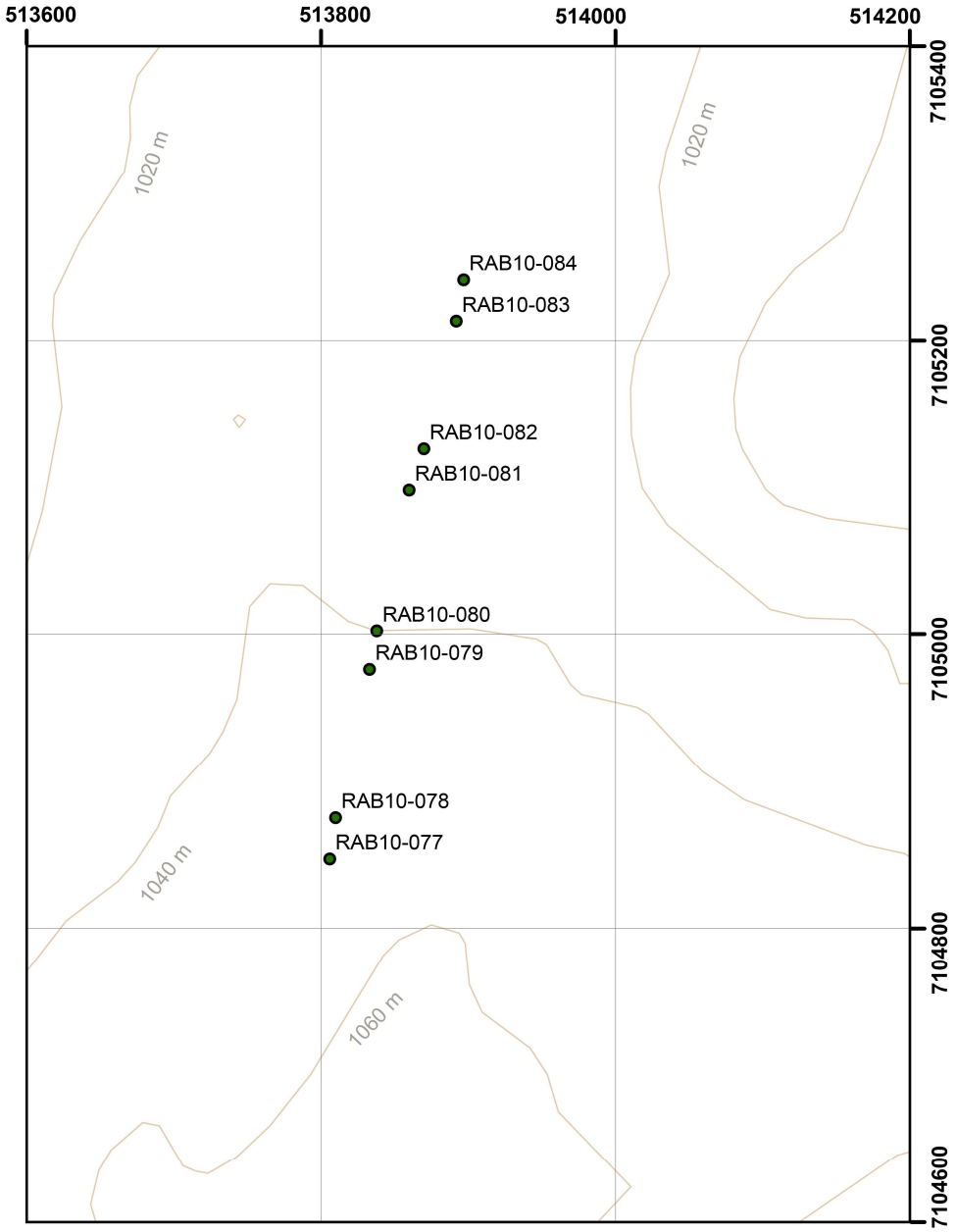

Figure S9. Drillhole location map H. Refer to Supplementary Figure S1. for this map's location within the Sixtymile District.

Figure S10. DDH-11-18 core samples, identified as medium-grained, quartz-rich quartz muscovite schists, which were measured for magnetic susceptibility.

Figure S11. DDH-11-15 core samples, identified as strongly foliated, fine- to coarse-grained muscovite quartz schists, measured for magnetic susceptibility.

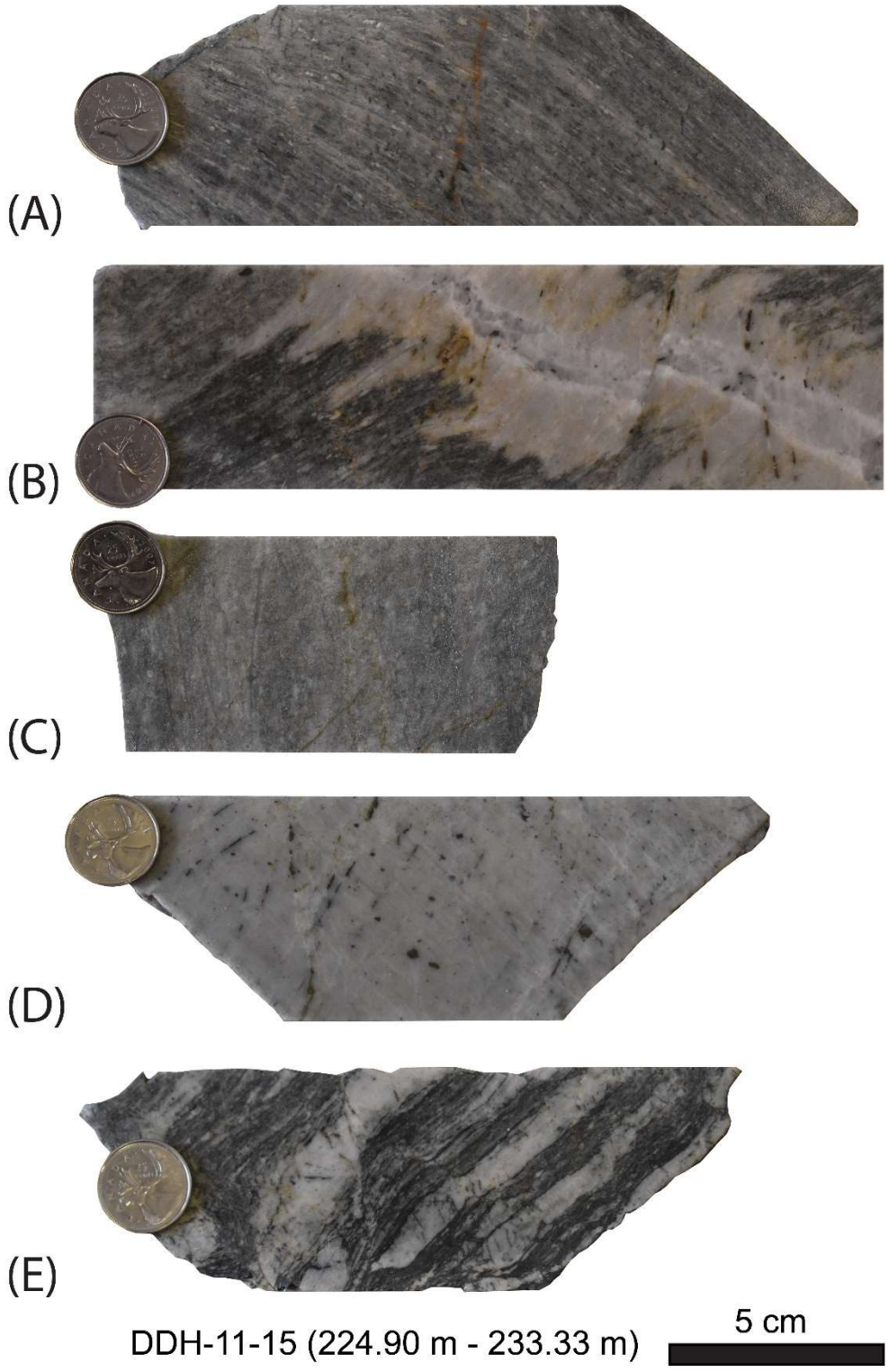

Figure S12. DDH-11-15 core samples, identified as strongly foliated, fine- to coarse-grained muscovite quartz schists, measured for magnetic susceptibility.

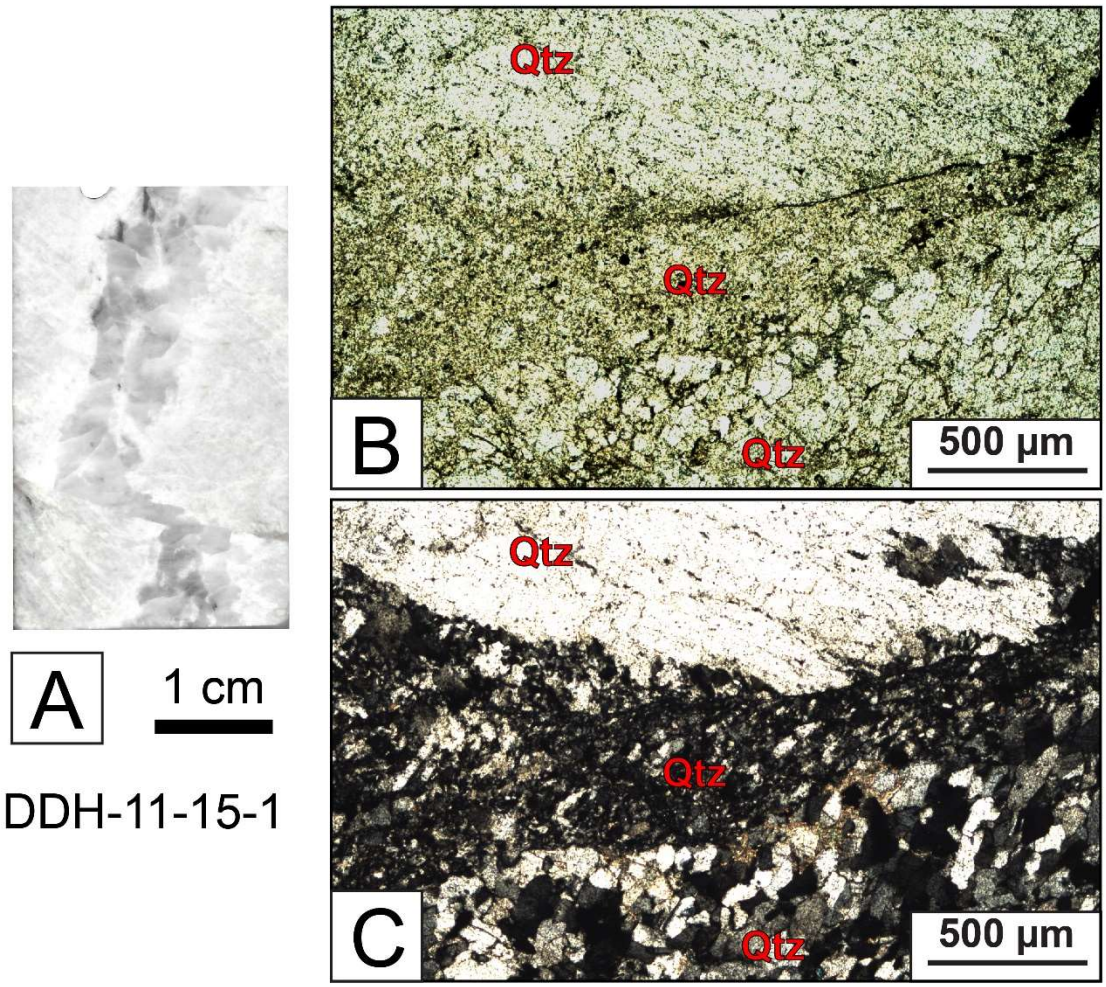

Figure S13. Thin section view of DDH-11-15-1, a strongly foliated, fine- to coarse-grained muscovite quartz schist taken from sample shown in Figure 19B. This sample shows offset of two generations of quarts veins. A) Hand sample from which thin section was prepared. B) Plane polarized light view. C) Cross polarized light view. 3 regions of quartz with different textures can be observed from top to bottom on the thin section views in Figure 20A&B: 1) > 1-mm-diameter, coarser crystals belonging to the younger, thinner quartz vein; 2) <50-µm-diameter, fine quartz fault gouge; 3) ~100-µm-diameter crystals belonging to the older quartz vein. Qtz—quartz.

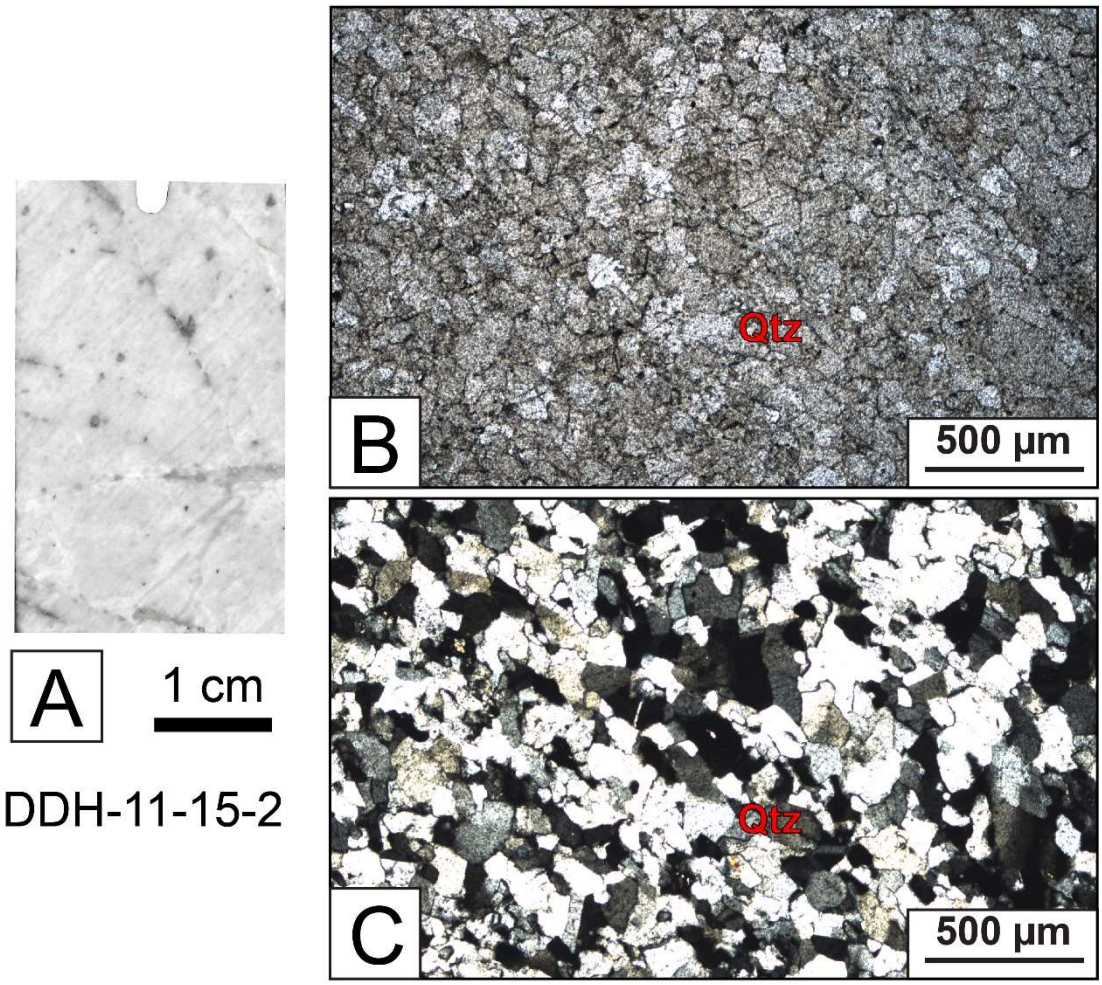

Figure S14. Thin section view of DDH-11-15-2, a strongly foliated, fine- to coarse-grained muscovite quartz schist taken from sample shown in Figure 19D. Quartz appear to have undergone recrystallization as evidenced by grain boundary migration. A) Hand sample from which thin section was prepared. B) Plane polarized light view. C) Cross polarized light view. D) Transmitted light view. Qtz—quartz

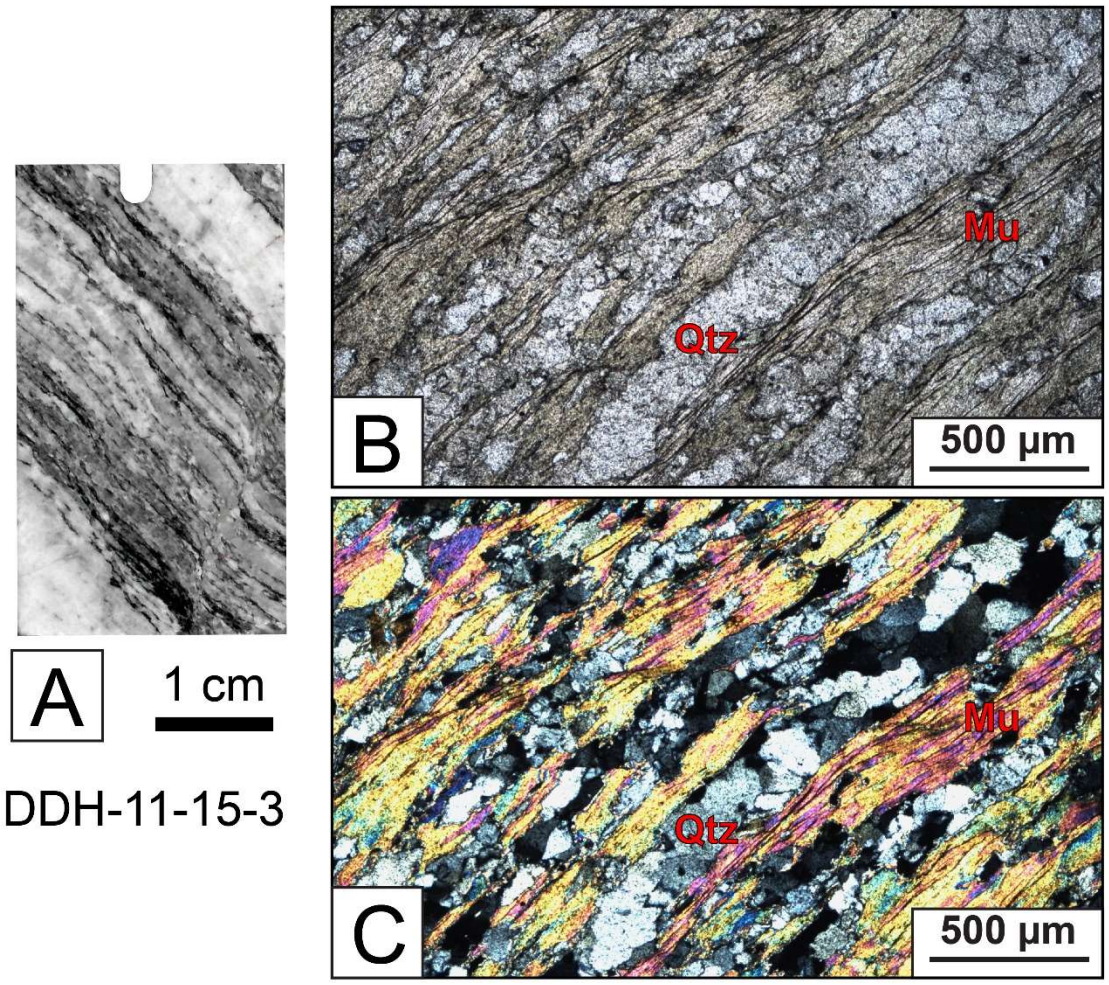

Figure S15. Thin section view of DDH-11-15-3, a strongly foliated, fine- to coarse-grained muscovite quartz schist taken from sample shown in Figure 19E. Alternating layers of mica and quartz crystals with an evident preferred orientation can be observed. A) Hand sample from which thin section was prepared. B) Plane polarized light view. C) Cross polarized light view. Qtz—quartz, Mu—muscovite.

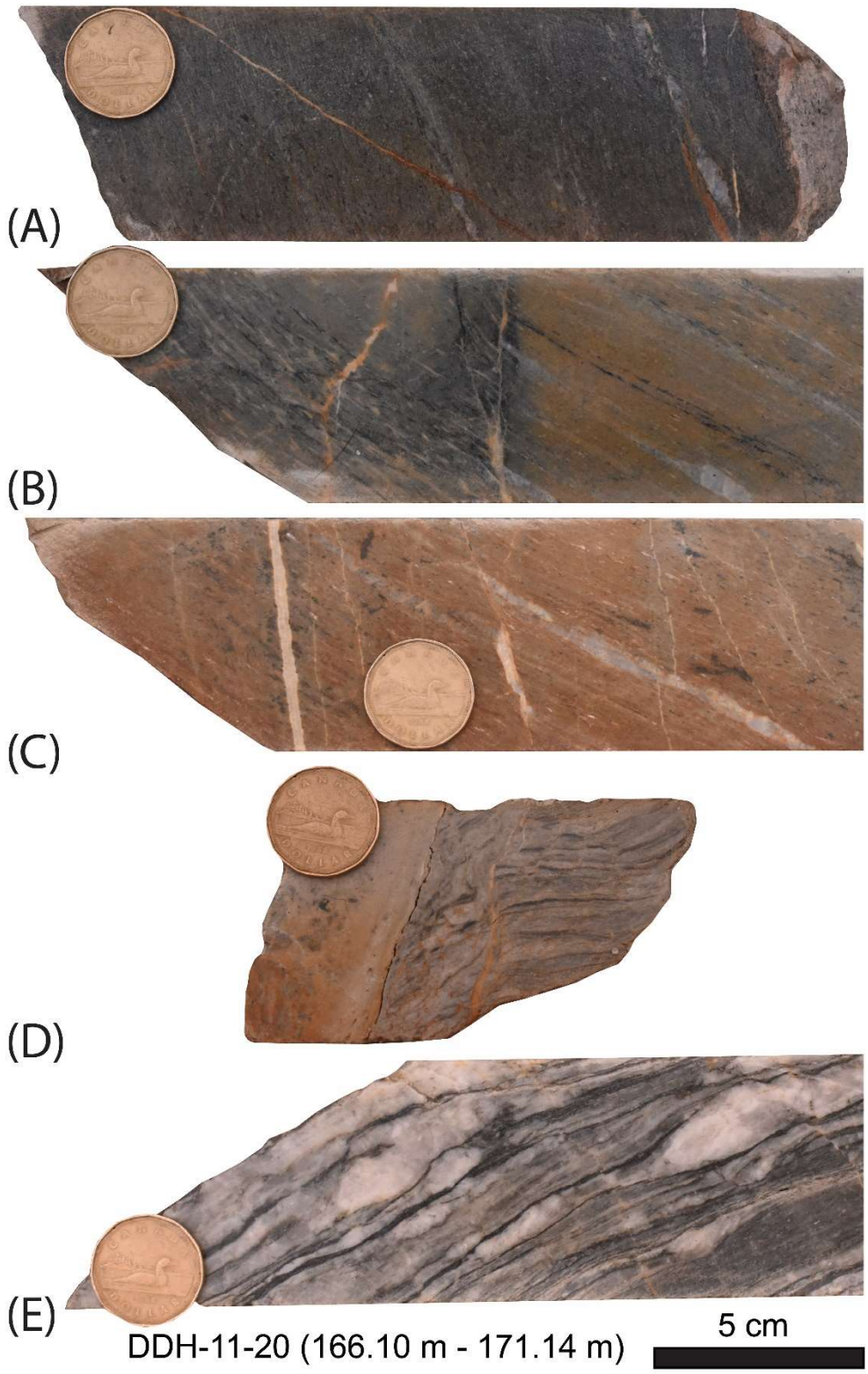

Figure S16. DDH-11-20 core samples, strongly foliated, fine- to coarse-grained muscovite quartz schists, measured for magnetic susceptibility.

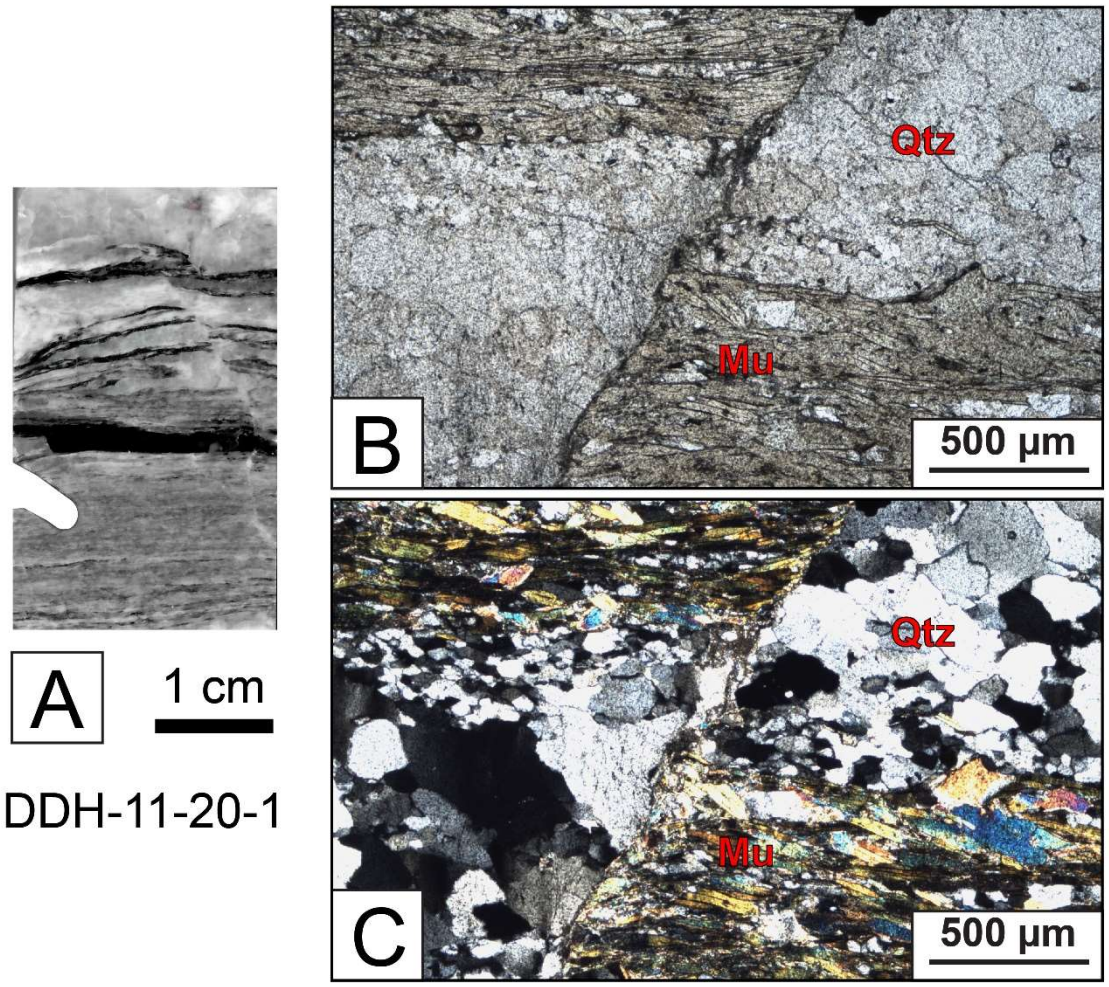

Figure S17. Thin section view of DDH-11-20-1, a strongly foliated, fine- to coarse-grained muscovite quartz schist. This samples exhibits faulted alternating layers of mica and quartz crystals. A) Hand sample from which thin section was prepared. B) Plane polarized light view. C) Cross polarized light view. Qtz—quartz, Mu—muscovite.

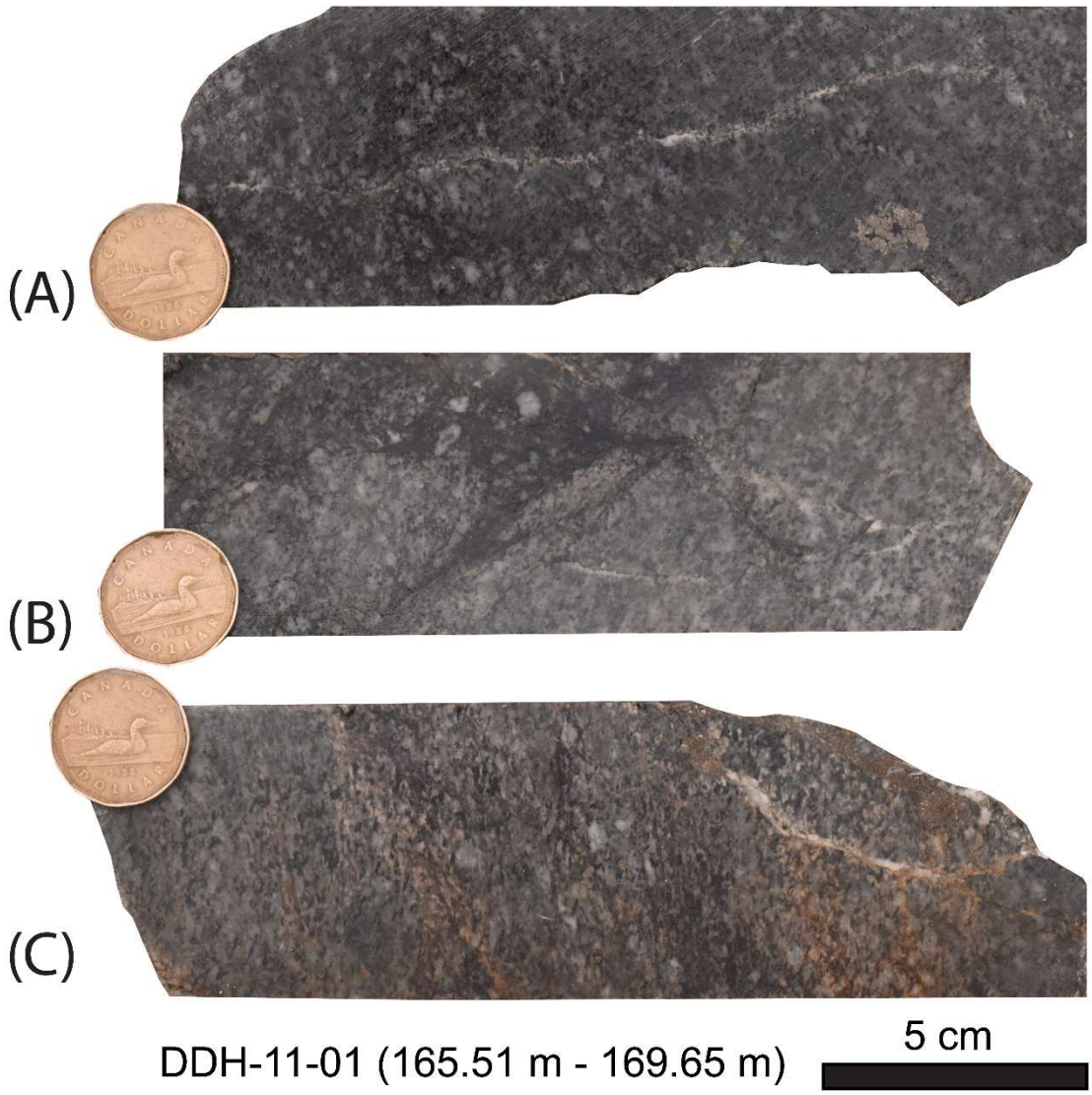

Figure S18. DDH-11-01 core samples, identified as generally medium-grained schists (with variety of compositions), measured for magnetic susceptibility.

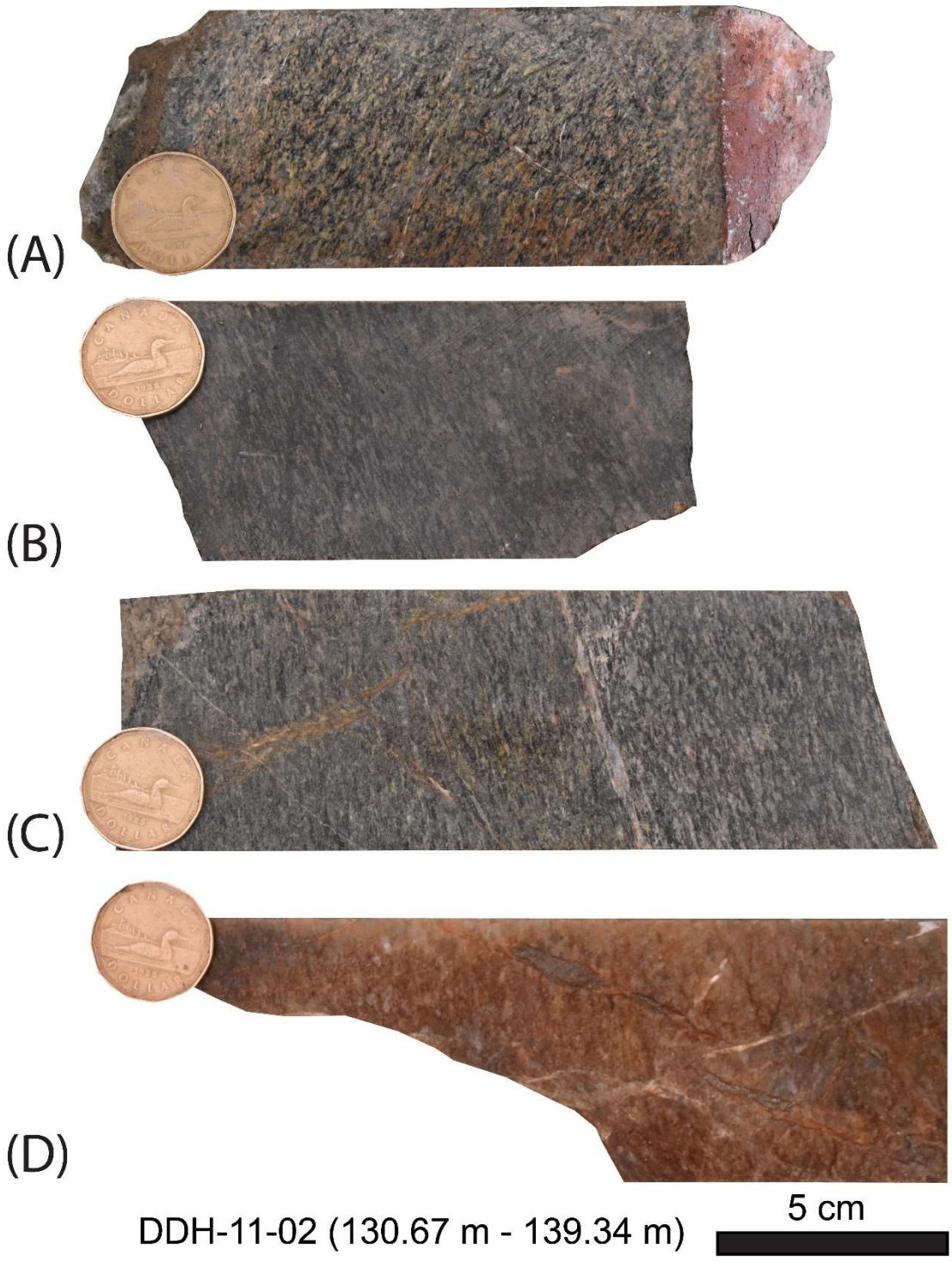

Figure S19. DDH-11-02 core samples, identified as chlorite-mica schists, measured for magnetic

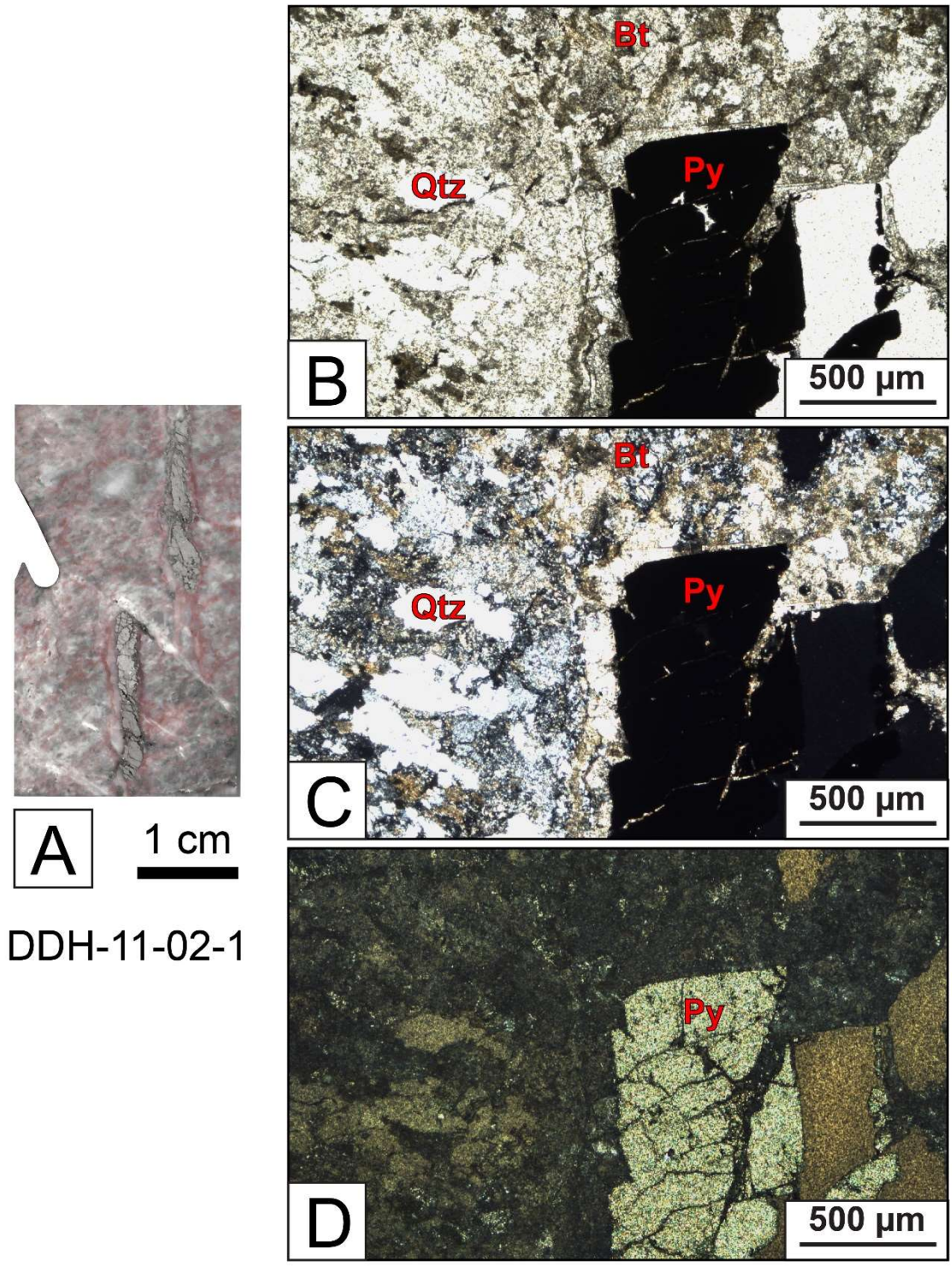

susceptibility.

Figure S20. Thin section view of DDH-11-02-1, a highly-altered chlorite-mica schist with stinger-related sulfide mineralization (e.g., pyrite). A) Hand sample from which thin section was prepared. B) Plane polarized light view. C) Cross polarized light view. D) Transmitted light view. Qtz—quartz, Bt—biotite, Py—pyrite.

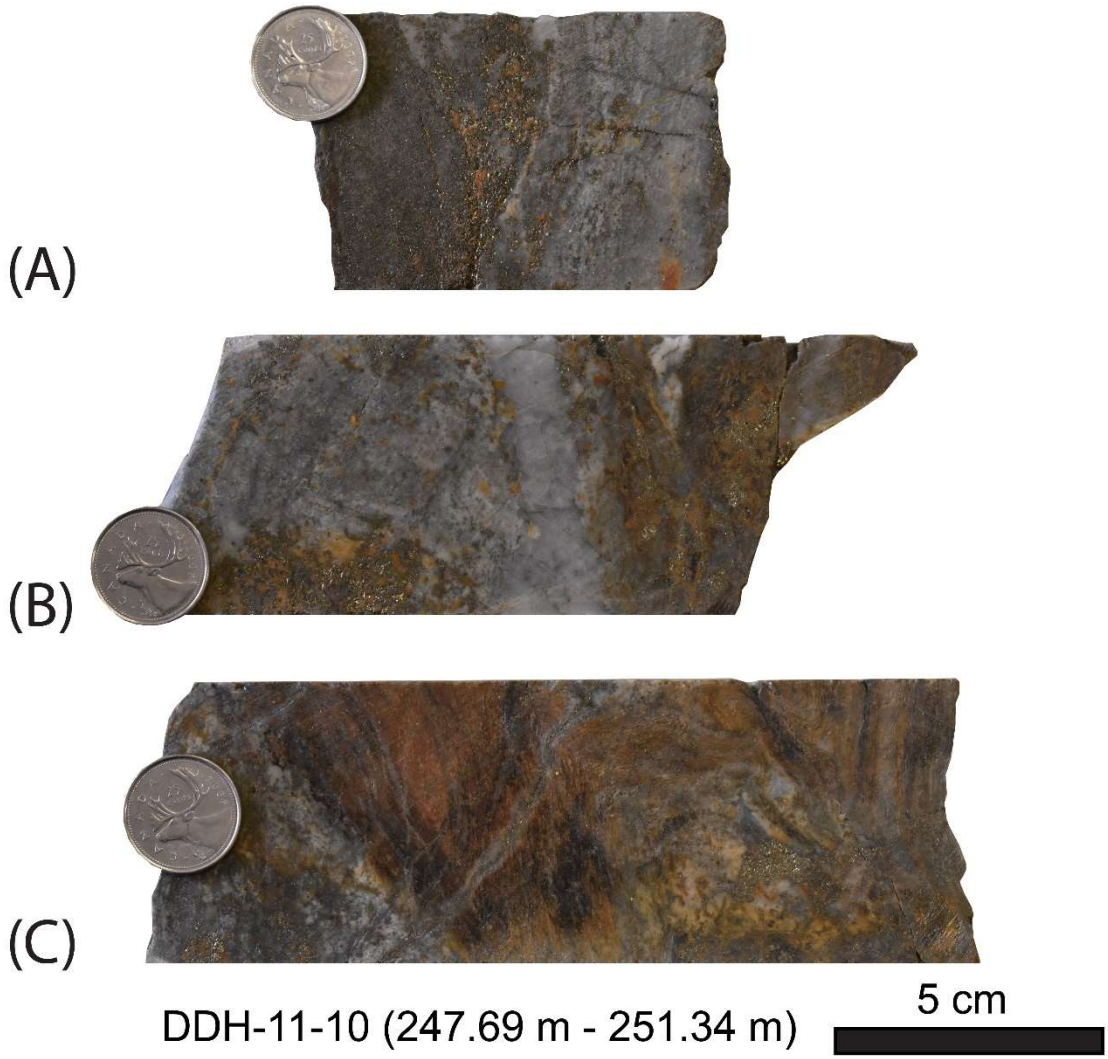

Figure S21. DDH-11-10 core samples, identified as quartz-biotite schists, measured for magnetic susceptibility.

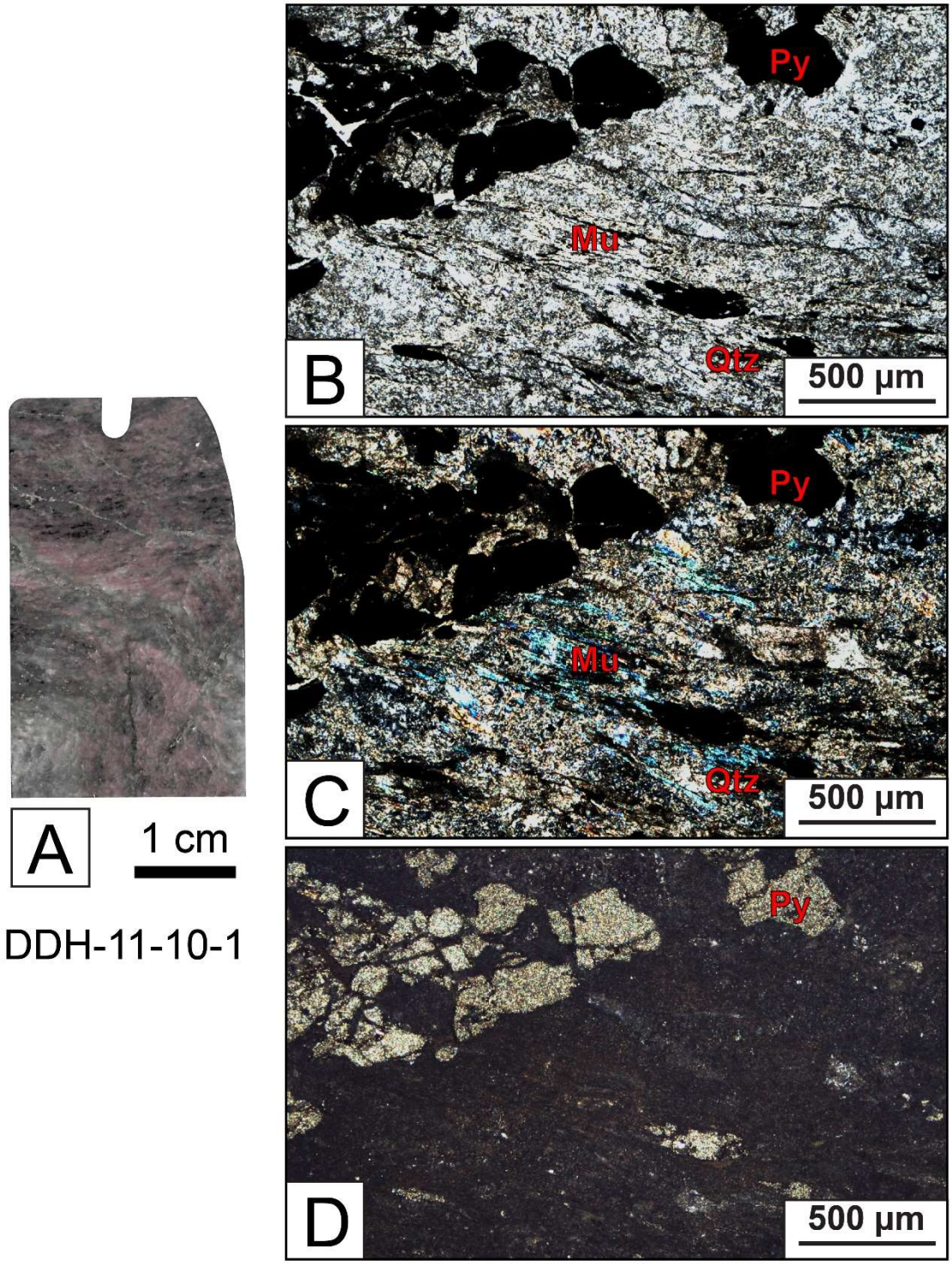

Figure S22. Thin section view of DDH-11-10-1, a quartz-mica schist which contains disseminated pyrite. A) Hand sample from which thin section was prepared. B) Plane polarized light view. C) Cross polarized light view. D) Transmitted light view. Qtz—quartz, Mu—muscovite, Py—pyrite.

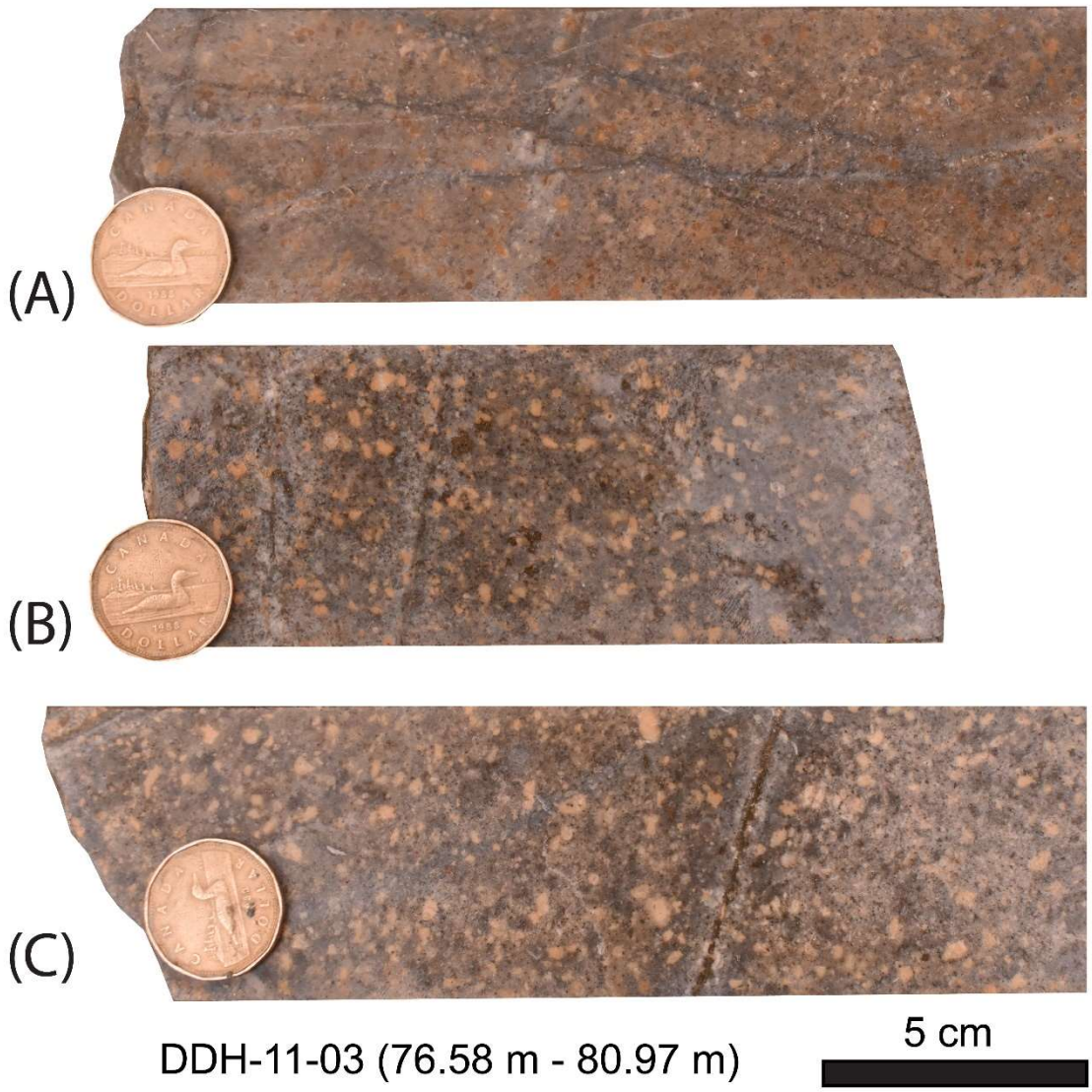

Figure S23. DDH-11-03 core samples, identified as fine- to coarse-grained porphyritic andesites, measured for magnetic susceptibility.

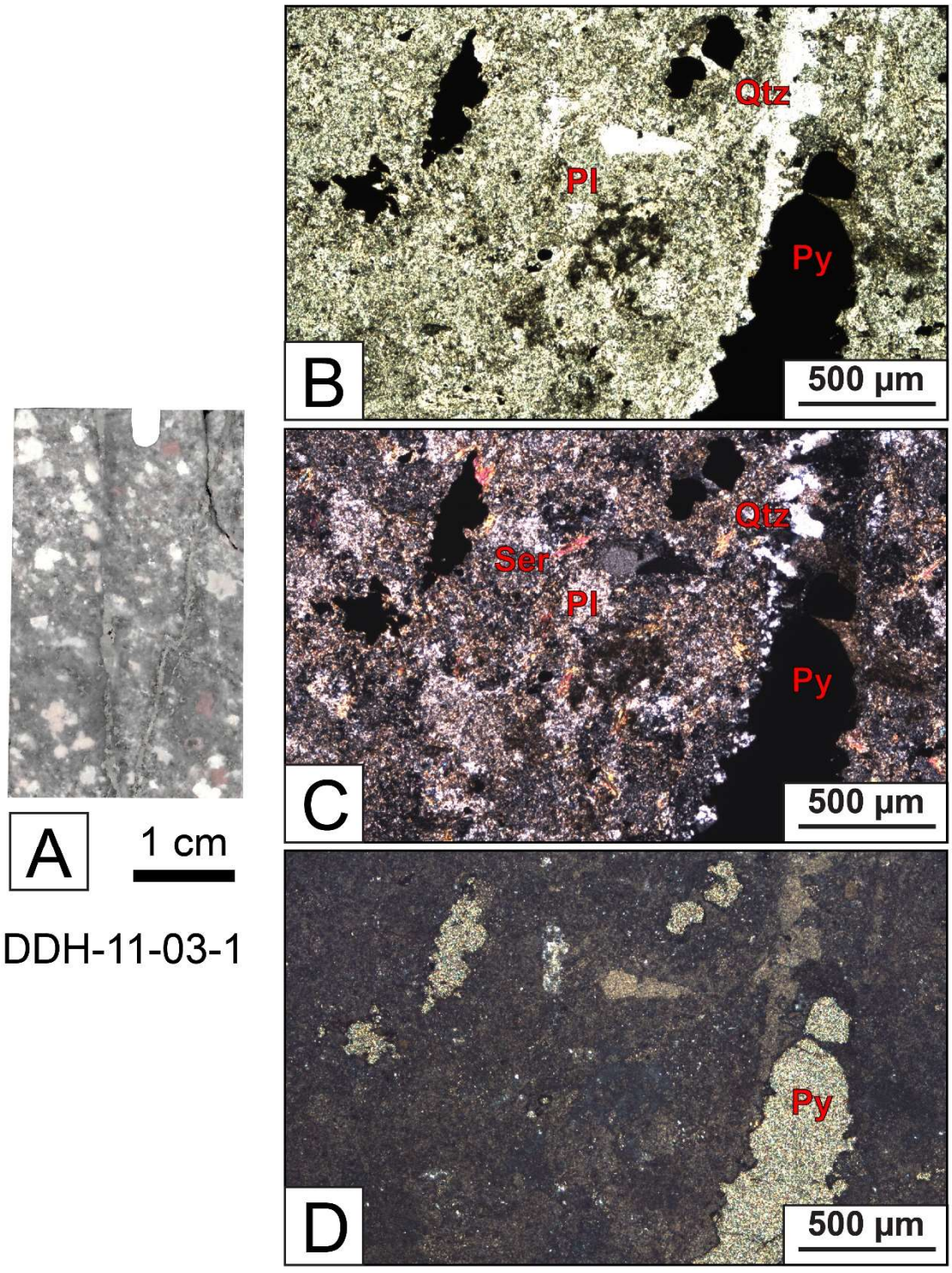

Figure S24. Thin section view of DDH-11-03-1, a highly-altered, fine- to coarse-grained porphyritic andesite which contains stringer-related pyrite. A) Hand sample from which thin section was prepared. B) Plane polarized light view. C) Cross polarized light view. D) Transmitted light view. Qtz—quartz, Py—pyrite, Pl—plagioclase, Ser—sericitization.

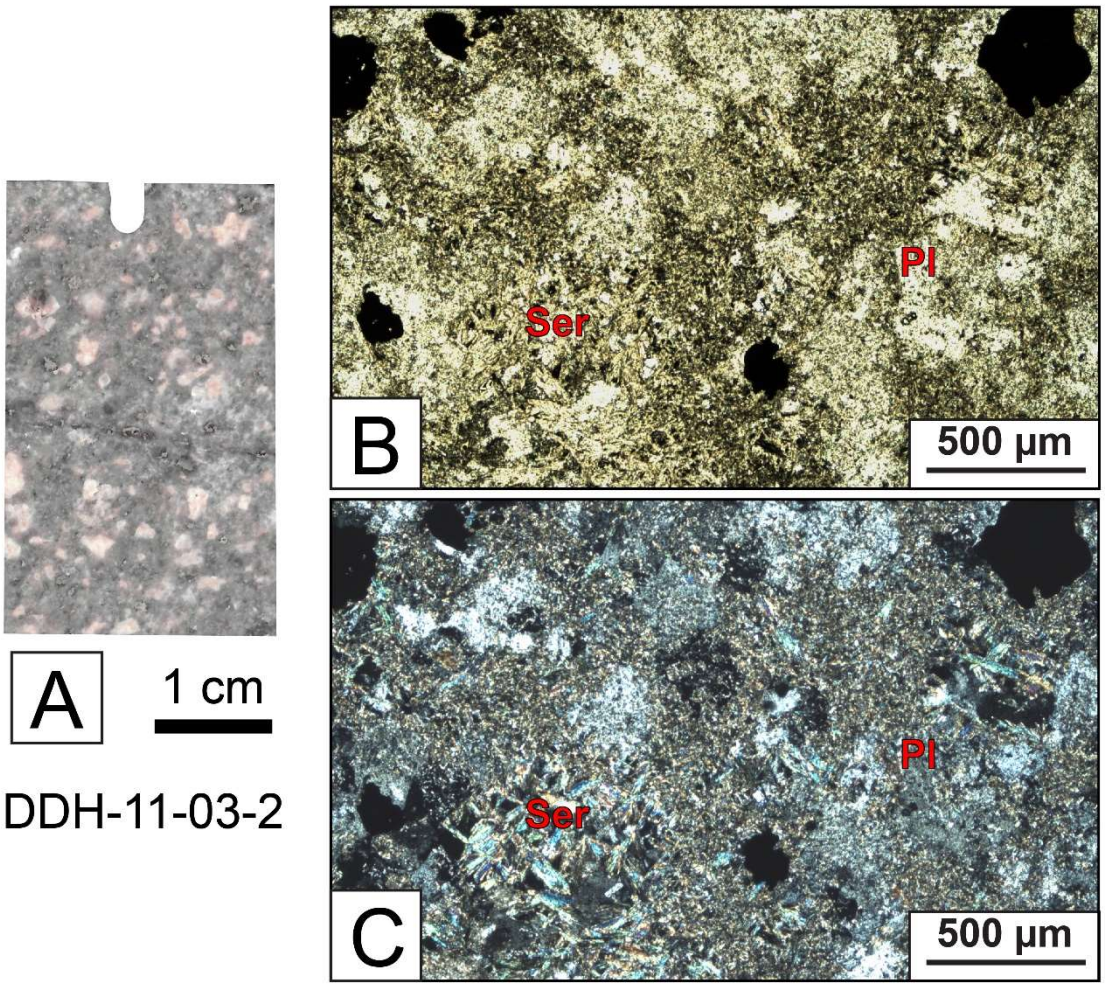

Figure S25. Thin section view of DDH-11-03-2, a highly-altered, fine- to coarse-grained porphyritic andesite. A) Hand sample from which thin section was prepared. B) Plane polarized light view. C) Cross polarized light view. Pl—plagioclase, Ser—sericitization.

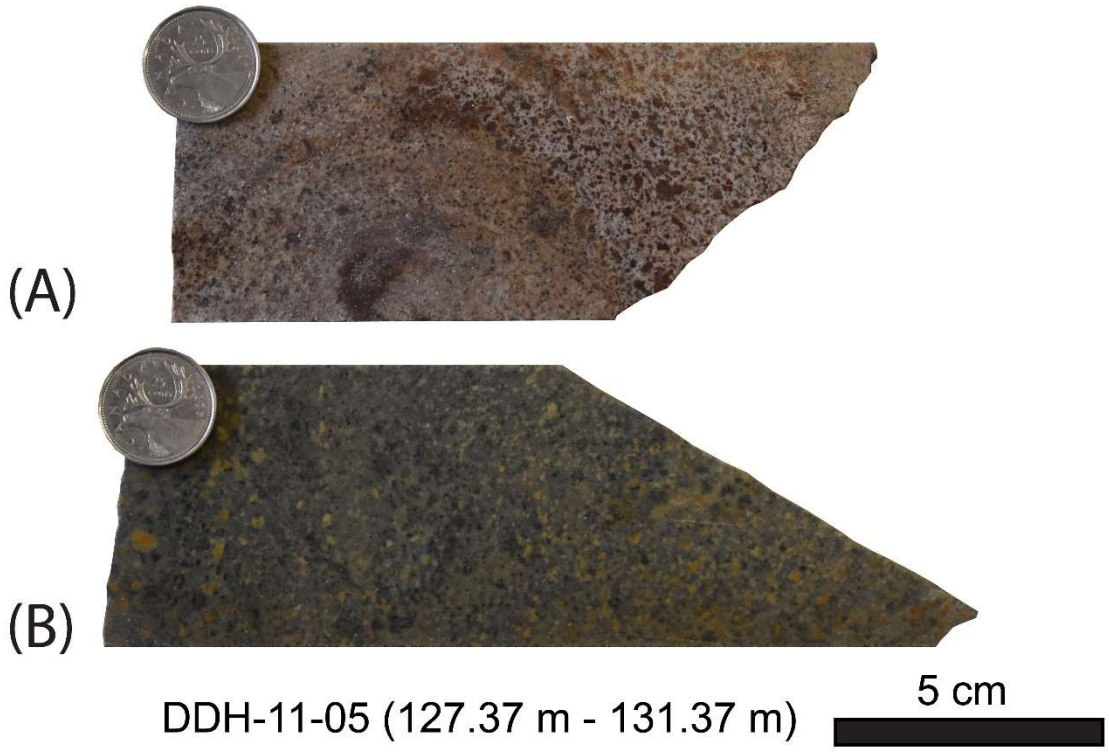

Figure S26. DDH-11-05 core samples, identified as fine- to coarse-grained porphyritic andesites, measured for magnetic susceptibility.

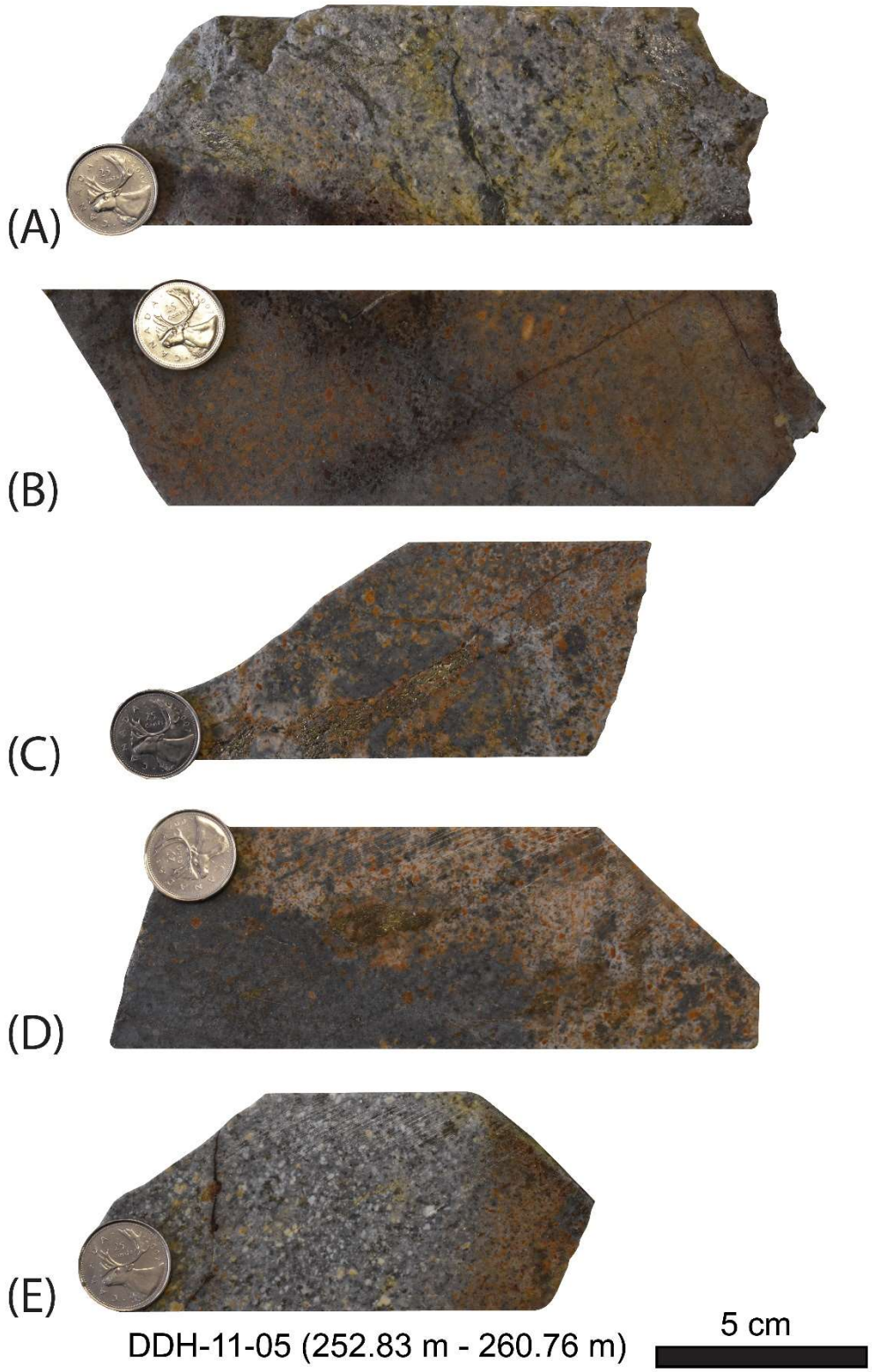

Figure S27. DDH-11-05 core samples, identified as fine- to coarse-grained porphyritic andesites, measured for magnetic susceptibility.

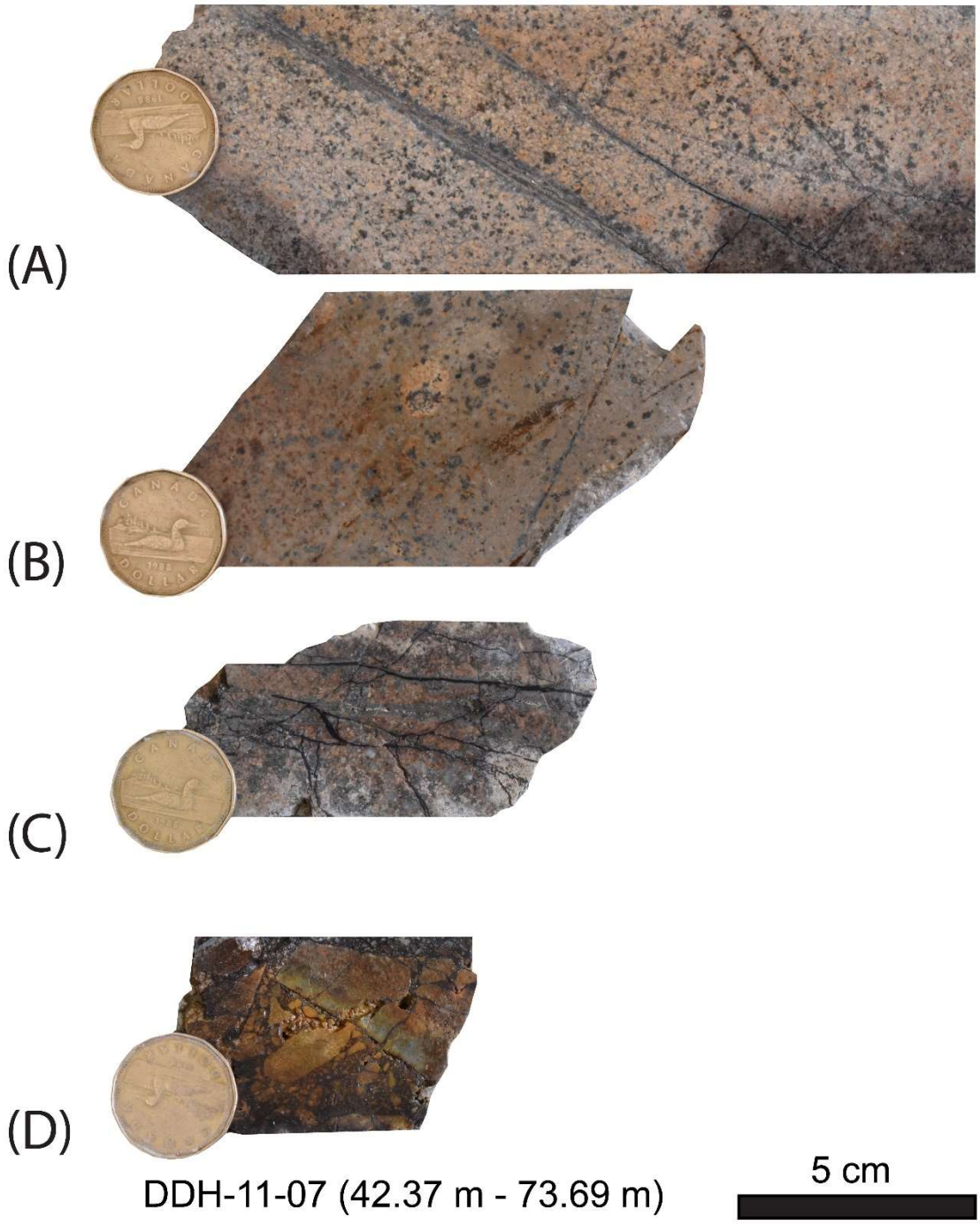

Figure S28. DDH-11-07 core samples, identified as fine- to coarse-grained porphyritic andesites, measured for magnetic susceptibility.

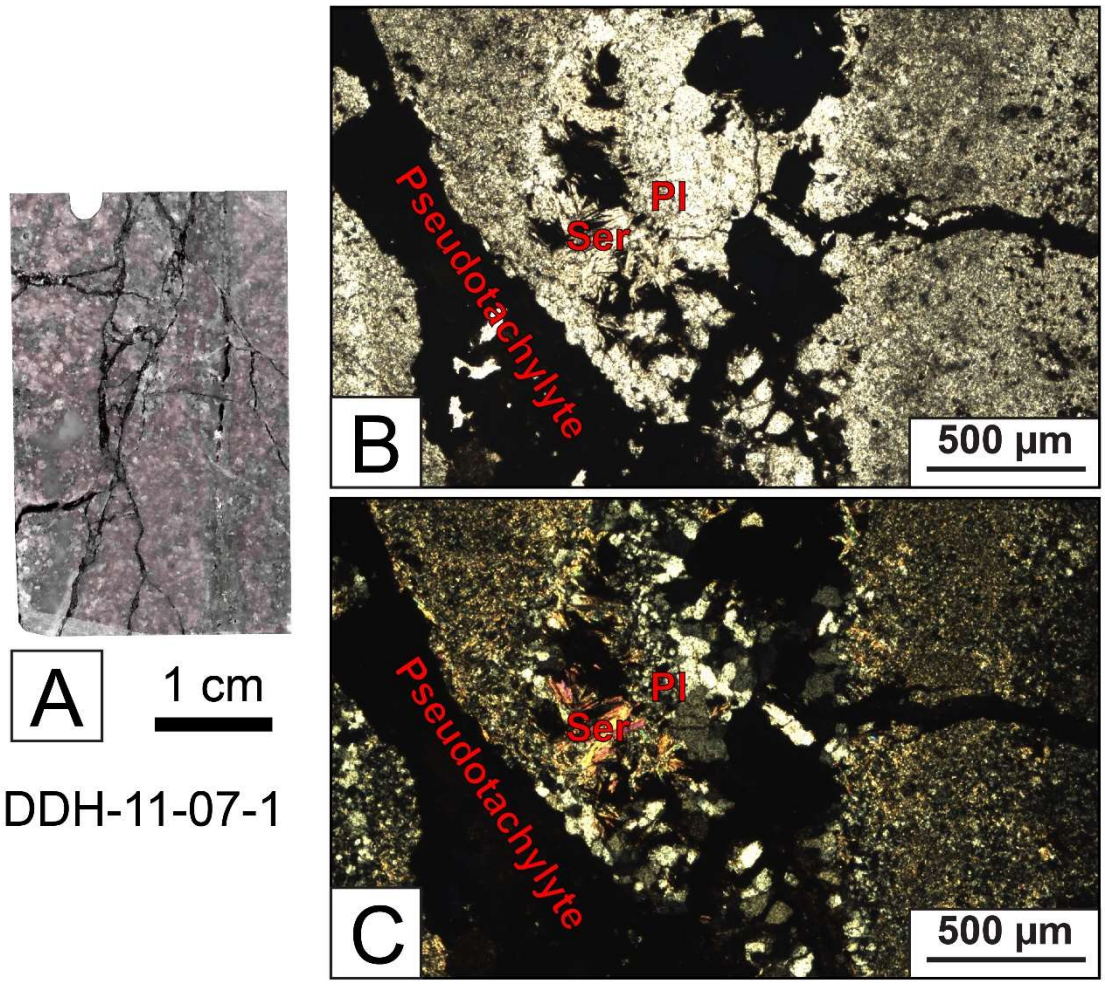

Figure S29. Thin section view of DDH-11-07-1, a fine- to coarse-grained porphyritic andesite exhibiting fault-generated pseudotachylyte. A) Hand sample from which thin section was prepared. B) Plane polarized light view. C) Cross polarized light view. Pl—plagioclase, Ser—sericitization.

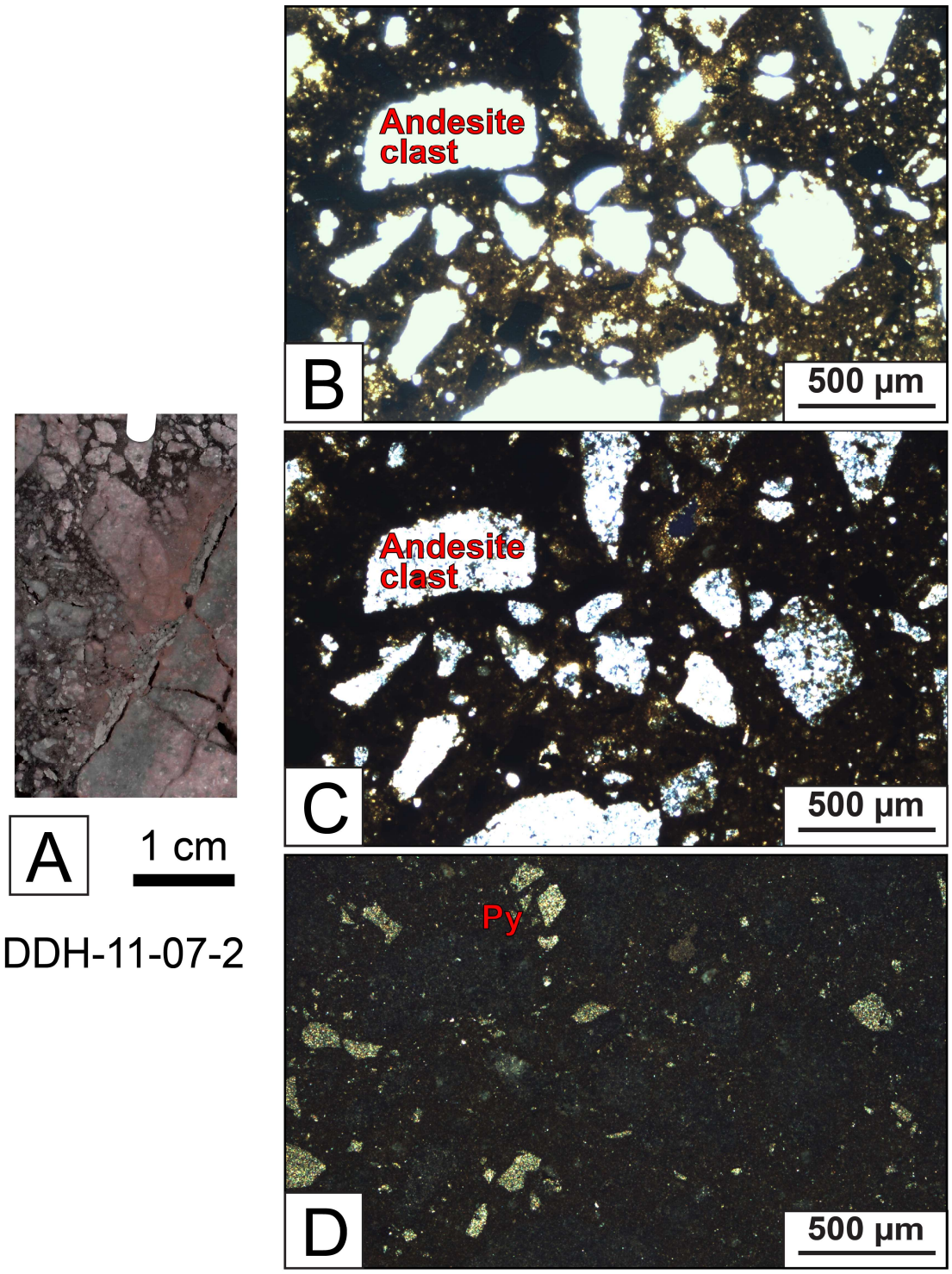

Figure S30. Thin section view of DDH-11-07-2, a brecciated fine- to coarse-grained porphyritic andesite. A) Hand sample from which thin section was prepared. B) Plane polarized light view. C) Cross polarized light view. D) Transmitted light view.

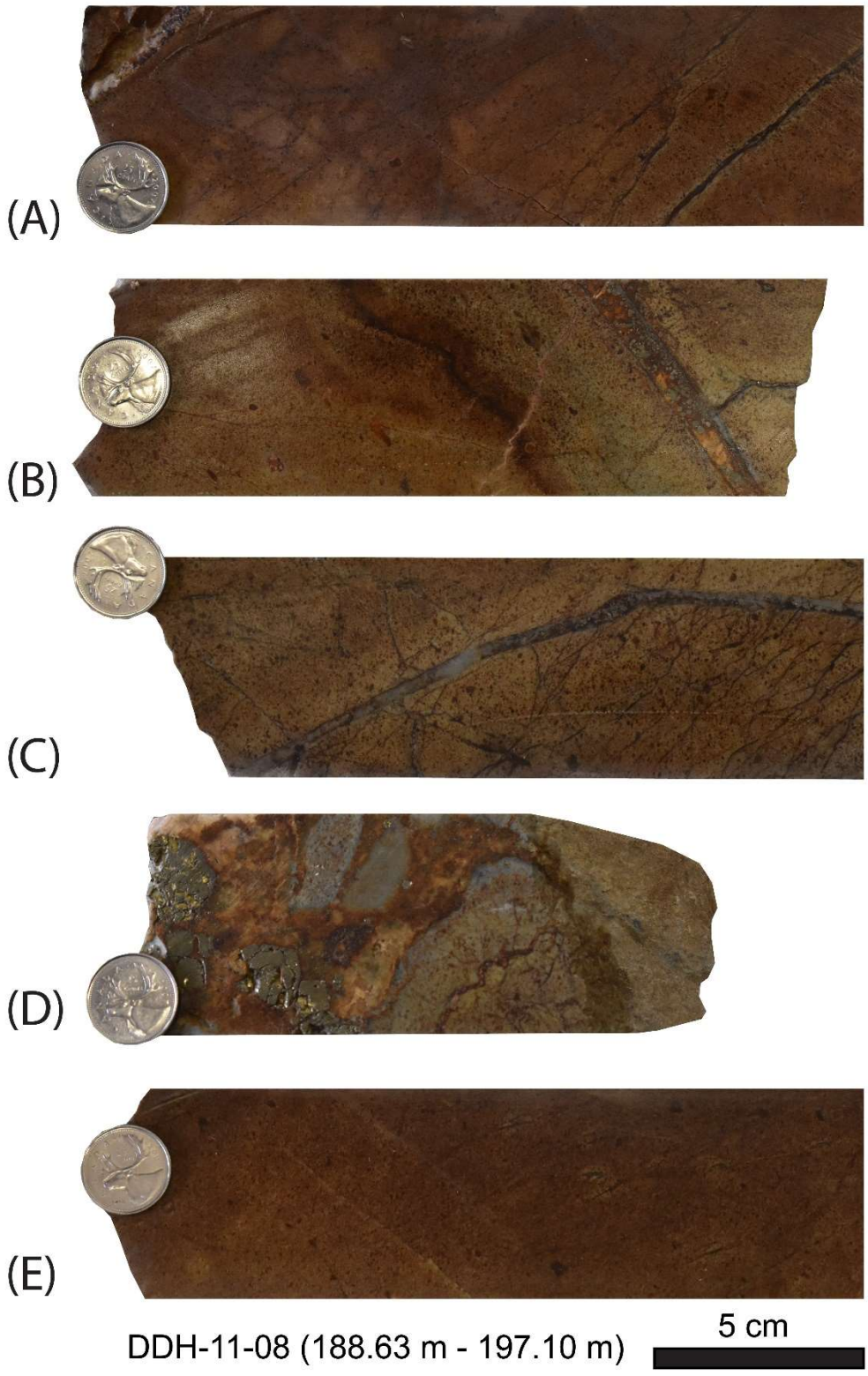

Figure S31. DDH-11-08 core samples, identified as fine- to coarse-grained porphyritic andesites, measured for magnetic susceptibility.

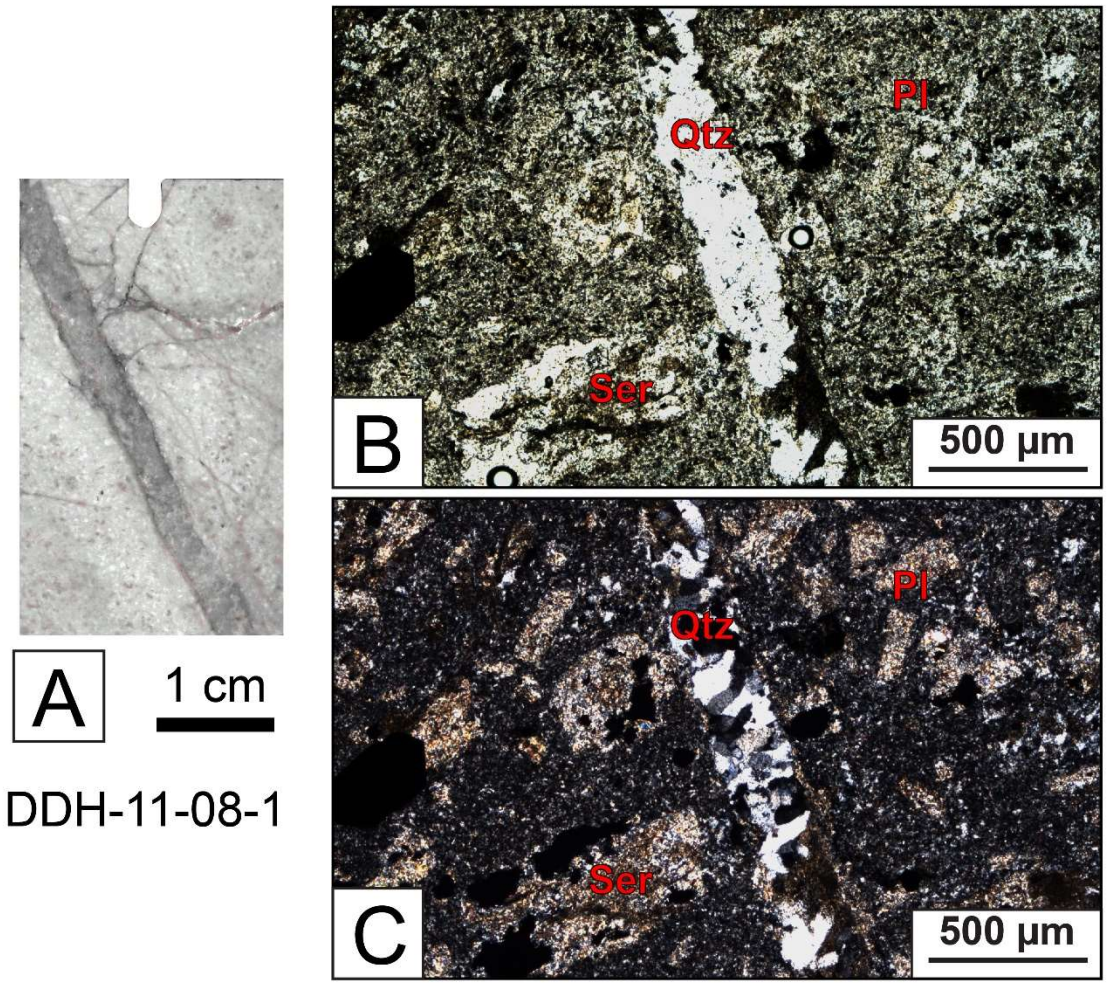

Figure S32. Thin section view of DDH-11-08-1, a fine- to coarse-grained porphyritic andesite. A) Hand sample from which thin section was prepared. B) Plane polarized light view. C) Cross polarized light view. Qtz—quartz, Pl—plagioclase, Ser—sericitization.

Figure S33. DDH-11-16 core samples, identified as fine- to coarse-grained porphyritic andesites, measured for magnetic susceptibility.

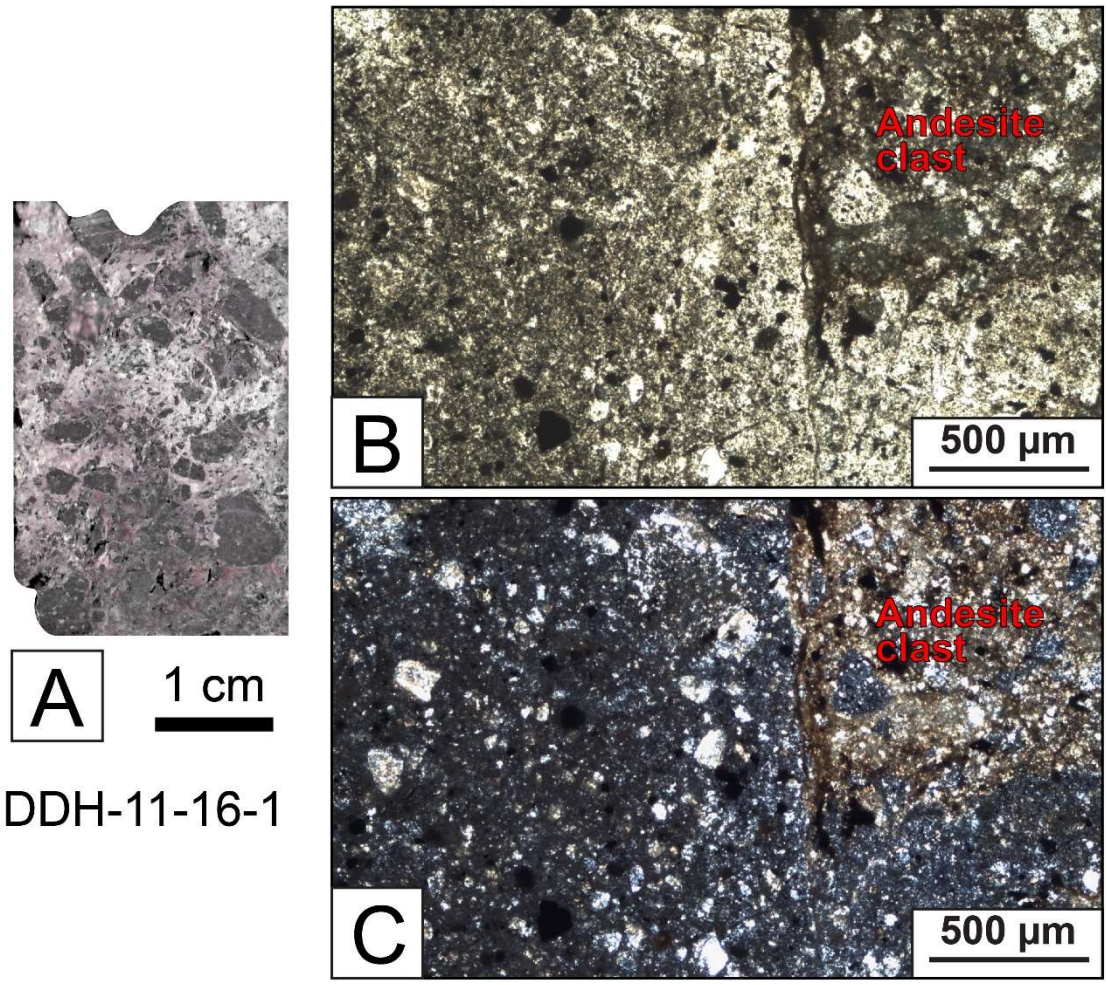

Figure S34. Thin section view of DDH-11-16-1, a brecciated fine- to coarse-grained porphyritic andesite. A) Hand sample from which thin section was prepared. B) Plane polarized light view. C) Cross polarized light view.

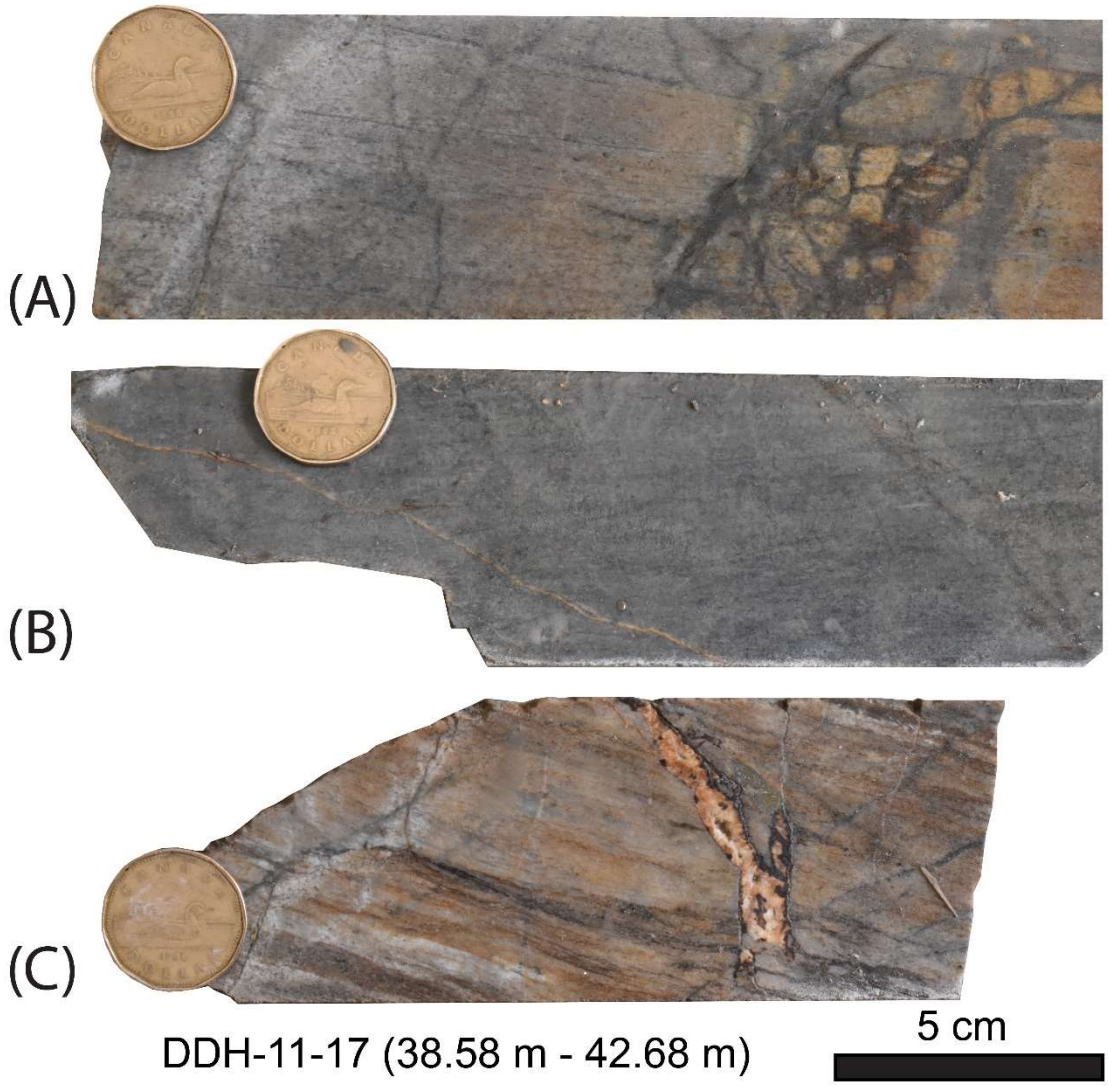

Figure S35. DDH-11-17 core samples, identified as fine- to coarse-grained porphyritic andesites, measured for magnetic susceptibility.

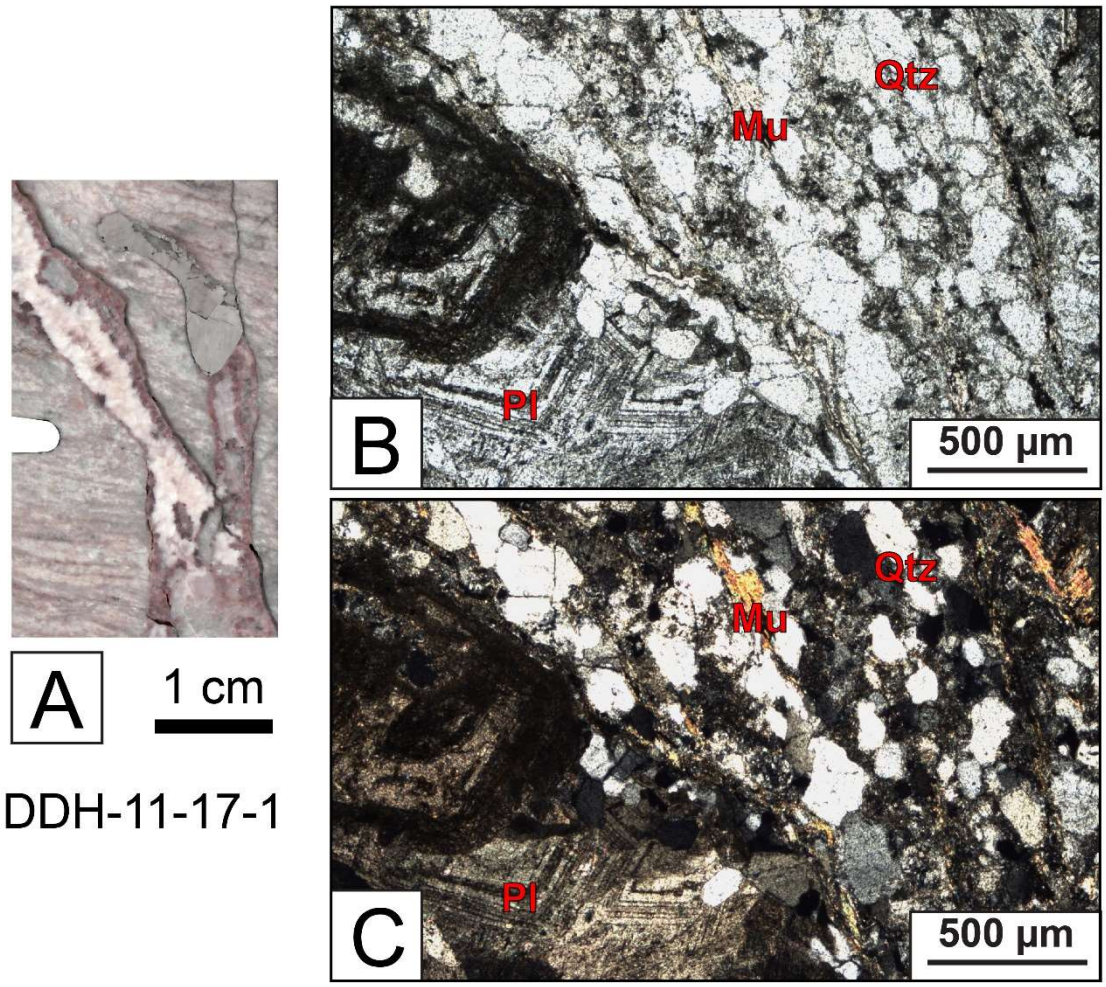

Figure S36. Thin section view of DDH-11-17-1, a fine- to coarse-grained porphyritic andesite. A) Hand sample from which thin section was prepared. B) Plane polarized light view. C) Cross polarized light view. Qtz—quartz, Mu—muscovite, Pl—plagioclase.

Table S1. Magnetic susceptibility drillhole measurements.

Drillhole Name	Approximate Depth (m)	Measurements (10^{-3} SI)	Lithology	Figure
DDH-11-01	165.91	0.7, 0.9, 0.9	Schist	Figure 25A
DDH-11-01	168.15	0.7, 0.6, 0.9	Schist	Figure 25B
DDH-11-01	169.1	0.5, 0.6, 0.7	Schist	Figure 25C
DDH-11-02	131.67	1.9, 1.9, 2	Chlorite-Mica Schist	Figure 26A
DDH-11-02	132.97	3.5, 3.5, 4.2	Chlorite-Mica Schist	Figure 26B
DDH-11-02	134.34	2.9, 2.9, 3.2	Chlorite-Mica Schist	Figure 26C
DDH-11-02	137.78	0.5, 0.5, 0.5	Chlorite-Mica Schist	Figure 26D
DDH-11-03	77.58	0.3, 0.3, 0.3	Andesite (Porphyritic)	Figure 30A
DDH-11-03	79.53	0.2, 0.2, 0.3	Andesite (Porphyritic)	Figure 30B
DDH-11-03	80.68	0.2, 0.2, 0.2	Andesite (Porphyritic)	Figure 30C
DDH-11-05	129.37	0.6, 0.6, 0.7	Andesite	Figure 33A
DDH-11-05	131.47	2.2, 2, 2.3	Andesite	Figure 33B
DDH-11-05	254.43	0, 0, 0	Andesite	Figure 34A
DDH-11-05	255.98	0.3, 0.4, 0.4	Andesite	Figure 34B
DDH-11-05	256.73	0.2, 0.2, 0.2	Andesite	Figure 34C
DDH-11-05	257.48	1.1, 1.3, 0.9	Andesite	Figure 34D
DDH-11-05	258.48	0, 0, 0.1	Andesite	Figure 34E
DDH-11-07	43.97	0.3, 0.3, 0.3	Andesite	Figure 35A
DDH-11-07	45.02	0.4, 0.4, 0.4	Andesite	Figure 35B
DDH-11-07	72.99	0.6, 0.5, 0.6	Andesite	Figure 35C
DDH-11-07	73.59	0.9, 0.8, 0.6	Andesite	Figure 35D
DDH-11-08	191.88	0.8, 0.9, 0.9	Andesite	Figure 36A
DDH-11-08	192.98	1.1, 1.2, 1.1	Andesite	Figure 36B
DDH-11-08	193.78	0.8, 1, 1.2	Andesite	Figure 36C
DDH-11-08	194.33	1.5, 1.6, 1.9	Andesite	Figure 36D
DDH-11-08	197.28	0.6, 0.8, 0.9	Andesite	Figure 36E
DDH-11-10	249.14	0.3, 0.3, 0.4	Quartz-Biotite Schist	Figure 28A
DDH-11-10	249.54	0.1, 0.2, 0.2	Quartz-Biotite Schist	Figure 28B
DDH-11-10	249.84	0.4, 0.4, 0.4	Quartz-Biotite Schist	Figure 28C
DDH-11-15	195.59	0, 0, 0	Muscovite Schist	Figure 18A
DDH-11-15	198.5	0.3, 0.3, 0.4	Muscovite Schist	Figure 18B
DDH-11-15	225.45	0.2, 0.2, 0.2	Muscovite Schist	Figure 19A
DDH-11-15	228.3	0.1, 0.2, 0.3	Muscovite Schist	Figure 19B
DDH-11-15	229.8	0.2, 0.2, 0.2	Muscovite Schist	Figure 19C
DDH-11-15	231.15	0, 0, 0	Muscovite Schist	Figure 19D
DDH-11-15	233.6	0.3, 0.2, 0.2	Muscovite Schist	Figure 19E
DDH-11-16	78.73	1.3, 1.2, 1.3	Breccia	Figure 40A
DDH-11-16	79.23	1.1, 1.2, 1.5	Breccia	Figure 40B
DDH-11-17	40.73	0.3, 0.3, 0.3	Andesite	Figure 42A
DDH-11-17	41.58	0.5, 0.5, 0.5	Andesite	Figure 42B
DDH-11-17	42.58	0.9, 0.9, 0.7	Andesite	Figure 42C
DDH-11-18	104.52	0.2, 0.3, 0.2	Quartz-Muscovite Schist	Figure 17A
DDH-11-18	105.35	0.1, 0.1, 0.1	Quartz-Muscovite Schist	Figure 17B
DDH-11-20	166.35	1.1, 1.2, 1.1	Chlorite-Biotite-Quartz Schist	Figure 23A

DDH-11-20	167.35	0.4, 0.4, 0.5	Chlorite-Biotite-Quartz Schist	Figure 23B
DDH-11-20	167.55	1.2, 1.2, 1.3	Chlorite-Biotite-Quartz Schist	Figure 23C
DDH-11-20	168.38	0.2, 0.3, 0.4	Chlorite-Biotite-Quartz Schist	Figure 23D
DDH-11-20	169.82	0.3, 0.4, 0.3	Chlorite-Biotite-Quartz Schist	Figure 23E

Table S2. Selected Gold Assay results in the Sixtymile district.

Drill Hole	Easting	Northing	From (m)	To (m)	Length (m)	Au (g/t)
SM21-09	506724	7097078	38.1	60.96 (EOH)	22.8	0.38
			56.4	60.96	4.57	1.04
SM21-10	506733	7097114	26	30.57	4.57	0.22
			50.3	60.97 (EOH)	10.67	0.74
SM21-11	506681	7097066	16.7	42.6	25.9	0.35
			16.7	22.9	6.1	1.02
			57.9	61	3.1	0.46
SM21-12	506702	7097085	6.1	36.6	33.5	0.45
			22.9	24.4	7.6	1.02
			54.9	61 (EOH)	6.1	0.75
DDH-10-01	506687	7097093	10	32	22	0.44
			10.67	17.8	7.13	0.76
			187	196.8	9.8	0.99
DDH-10-02	506734	7097073	35	75.8	40.8	0.63
			41.15	43.28	1.5	12.7
			235	247.7	12.7	0.38
DDH-10-03	506779	7097167	35	45.7	10.7	0.45
			36.6	38.1	1.5	1.2
			58	63.6	5.6	0.66
			203	208	5	0.57
			243	250.6	7.6	0.5
DDH 11-15	506727	7097076	192	196.5	4.5	1.03
			232	249.9	17.9	0.5
			234	238	4	1.1
DDH 11-18	506465	7097260	106	193	87	0.69
			141.93	155	13.07	2.43

*Intercepts were partially re-assayed in 2020 with metallic screen. Intercepts are calculated using updated metallic screen and historical results.

*EOH = end of hole

*Samples for assay data were taken from historical drilling and June 2021 RAB drilling